

Fast implicit difference schemes for time-space fractional diffusion equations with the integral fractional Laplacian

Xian-Ming Gu^{a,c}, Hai-Wei Sun^{b,*}, Yanzhi Zhang^d, Yong-Liang Zhao^e

^a*School of Economic Mathematics/Institute of Mathematics,*

Southwestern University of Finance and Economics, Chengdu, Sichuan 611130, China

^b*Department of Mathematics, University of Macau, Avenida da Universidade, Taipa, Macao, China*

^c*Bernoulli Institute for Mathematics, Computer Science and Artificial Intelligence,
University of Groningen, Nijenborgh 9, P.O. Box 407, 9700 AK Groningen, The Netherlands*

^d*Department of Mathematics and Statistics,*

Missouri University of Science and Technology, Rolla, MO 65409-0020, United States

^e*School of Mathematical Sciences,*

University of Electronic Science and Technology of China, Chengdu, Sichuan 611731, China

Abstract

In this paper, we develop two fast implicit difference schemes for solving a class of variable-coefficient time-space fractional diffusion equations with integral fractional Laplacian (IFL). The proposed schemes utilize the graded $L1$ formula and a special finite difference discretization for the Caputo fractional derivative and IFL, respectively, where the graded mesh can capture the model problem with a weak singularity at initial time. The stability and convergence are rigorously proved via the M -matrix analysis, which is from the spatial discretized matrix of IFL. Moreover, the proposed schemes use the fast sum-of-exponential approximation and Toeplitz matrix algorithms to reduce the computational cost for the nonlocal property of time and space fractional derivatives, respectively. The fast schemes greatly reduce the computational work of solving the discretized linear systems from $\mathcal{O}(MN^3 + M^2N)$ by a direct solver to $\mathcal{O}(MN(\log N + N_{exp}))$ per preconditioned Krylov subspace iteration and a memory requirement from $O(MN^2)$ to $O(NN_{exp})$, where N and $(N_{exp} \ll) M$ are the number of spatial and temporal grid nodes. The spectrum of preconditioned matrix is also given for ensuring the acceleration benefit of circulant preconditioners. Finally, numerical results are presented to show the utility of the proposed methods.

Keywords: Fractional diffusion equations; Caputo derivative; Integral fractional Laplacian; Circulant preconditioner; Krylov subspace solvers.

*Corresponding author

Email addresses: guxianming@live.cn, guxm@swufe.edu.cn (Xian-Ming Gu), hsun@umac.mo (Hai-Wei Sun), zhangyanz@mst.edu (Yanzhi Zhang), ylzhaofde@sina.com (Yong-Liang Zhao)

1. Introduction

In recent decades, fractional partial differential equations (FPDEs) have attracted growing attention in modeling phenomena with nonlocality and spatial heterogeneity arising in engineering, physics, chemistry and other applied sciences [1, 2]. In physics, fractional derivatives are used to model anomalous diffusion. Anomalous diffusion is the theory of diffusing particles in environments that are not locally homogeneous [3–6]. A physical-mathematical model to anomalous diffusion may be based on FPDEs containing derivatives of fractional order in both space and time, where the sub-diffusion appears in time and the super-diffusion occurs in space simultaneously [7, 8]. On the other hand, although most of time-space fractional diffusion models are initially defined with the spatially integral fractional Laplacian (IFL) [9, 11–13], many previous studies (cf. e.g., [4, 5, 14–16]) always substitute the space Riesz fractional derivative [1] for the IFL. In fact, such two kinds of definitions are not equivalent in high-dimensional cases [12, 16, 17]. It means that the ‘direct’ study of time-space fractional diffusion models with the IFL should be worthily considered.

In this paper, we study an alternative time-space fractional diffusion equation (TSFDE) with variable coefficients in one space dimension

$$\begin{cases} {}_0^C D_t^\gamma u(x, t) = -\kappa(x, t)(-\Delta)^{\alpha/2} u(x, t) + f(x, t), & x \in \Omega, \quad t \in (0, T], \\ u(x, t) = 0, & x \in \Omega^c, \quad t \in [0, T], \\ u(x, 0) = \phi(x), & x \in \Omega \end{cases} \quad (1.1)$$

with a weak singularity at the initial time $t = 0$, where $\kappa(x, t) > 0$ denotes the diffusivity coefficients, $\Omega = (-l, l)$, $\Omega^c = \mathbb{R} \setminus \Omega$, and the initial condition $\phi(x)$ and the source term $f(x, t)$ are known functions. Meanwhile, ${}_0^C D_t^\gamma$ is the Caputo derivative [1] of order γ - i.e.

$${}_0^C D_t^\gamma u(x, t) = \begin{cases} \frac{1}{\Gamma(\gamma-1)} \int_0^t \frac{1}{(t-s)^\gamma} \frac{\partial u(x, s)}{\partial s} ds, & 0 < \gamma < 1, \\ \frac{\partial u(x, t)}{\partial t}, & \gamma = 1, \end{cases} \quad (1.2)$$

and throughout the paper we always assume that $0 < \gamma < 1$. Here the fractional Laplacian $(-\Delta)^{\alpha/2}$ is defined by [9–12]:

$$(-\Delta)^{\alpha/2} u(x) = c_{1,\alpha} \text{P.V.} \int_{\mathbb{R}} \frac{u(x) - u(x')}{|x - x'|^{1+\alpha}} dx', \quad \alpha \in (0, 2), \quad (1.3)$$

where P.V. stands for the Cauchy principal value, and $|x - x'|$ denotes the Euclidean distance between points x and x' . The normalization constant $c_{1,\alpha}$ is defined as

$$c_{1,\alpha} = \frac{2^{\alpha-1} \alpha \Gamma(\frac{\alpha+1}{2})}{\sqrt{\pi} \Gamma(1 - \alpha/2)} \quad (1.4)$$

with $\Gamma(\cdot)$ denoting the Gamma function. From a probabilistic point of view, the IFL represents the infinitesimal generator of a symmetric α -stable Lévy process [12, 17, 18]. Mathematically, the well-posedness/regularity of the Cauchy problem or uniqueness of the solutions of the TSFDE (1.1) has been studied in [3, 19–23].

Due to the nonlocality, the analytical (or closed-form) solutions of TSFDEs (1.1) on a finite domain are rarely available. Therefore, we must rely on numerical treatments that produce approximations to the desired solutions; refer, e.g., to [1, 13, 24–26] and references therein for a description of such approaches. In fact, utilizing the suitable temporal discretization, most of the early established numerical methods including the finite difference (FD) method [8, 27–29], finite element (FE) method [30, 31], and matrix (named it as all-at-once) method [14, 32] for the TSFDE (1.1) were developed via the fact that the IFL is equivalent to the Riesz fractional derivative in one space dimension [15]. However, such a numerical framework cannot be directly extended to solve the two- and three-dimensional TSFDEs due to the IFL $(-\Delta)^{\alpha/2}u(x, y) \neq -\frac{\partial^\alpha u(x, y)}{\partial |x|^\alpha} - \frac{\partial^\alpha u(x, y)}{\partial |y|^\alpha}$ [12, 16, 17]. Therefore, it will distract the development of numerical solutions for TSFDEs from the stated objective.

In order to remedy the above drawback, Duo, Ju and Zhang [33] replace the IFL in TSFDE (1.1) by the spectral fractional Laplacian [12, 16] and present a fast numerical approach which combines the matrix transfer method [16] with inverse Laplace transform for solving the one- and multi-dimensional TSFDEs (1.1) with *constant coefficients*. Although the numerical results show that their proposed method converges with the second-order accuracy in both time and space variables, the spectral fractional Laplacian on a bounded domain is also not equivalent to the IFL at all [12]. On the other hand, Nochetto, Otárola and Salgado [53] use the Caffarelli-Silvestre extension to rewrite the TSFDE (1.1) with $\kappa(x, t) \equiv \kappa$ as a two-dimensional quasi-stationary elliptic problem with dynamic boundary condition. Then, they establish a FE scheme for solving the converted elliptic problem and show that the numerical scheme cannot reach the error estimates of order $O(\tau^{2-\gamma})$ claimed in the literature. Later, Hu, Li and Li [34, 35] successively exploit the similar strategy with FD approximation for the converted elliptic problem of one- and multi-dimensional TSFDEs (1.1 with $\kappa(x, t) \equiv \kappa$. Nevertheless, the numerical results show that such FD schemes often converge with the less than first- and second-order accuracy in time and space, respectively, even for TSFDEs with sufficient smooth solutions.

In fact, it is very essential to set up numerical schemes which utilize the ‘direct’ discretizations of IFL for solving the TSFDEs (1.1). Moreover, the discretizations of (multi-dimensional) become a recently hot topic, with the main numerical challenge stemming from the approximation the hypersingular integral, see e.g. [11, 36–43]. Indeed, there are some numerical schemes utilized the temporal $L1$ formula [44] (or numerical Laplace inversion [24]) and spatial FE discretization [11, 26, 40–42] for solving the (multi-dimensional) constant-coefficient TSFDEs (1.1) [7, 25, 26]. Both the theoretical and numerical results are reported to show that such numerical schemes are efficient to solve the (multi-dimensional) TSFDEs (1.1) with $\kappa(x, t) \equiv \kappa$. In addition, there are some other kinds of time-space fractional diffusion models but related to TSFDEs (1.1), where the spatial (or temporal) nonlocal operator is a replacement for the ILF (or the Caputo fractional derivative). This is mainly because the nonlocal operators with suitable kernels can exactly embrace the IFL and the Caputo fractional derivative, respectively [9, 11, 45–47]. For such novel model problems, Guan and Max [45] establish a class of numerical methods unitized the θ schemes and piecewise-linear FE discretization. Their fully discrete scheme is analyzed for all to determine conditional and unconditional stability regimes for the scheme and also to obtain error

estimates for the approximate solution. Later, Liu, et al. [46] improve the idea of Guan and Max by giving the proof of convergence behavior with $\mathcal{O}(\tau^{2-\gamma} + h^2)$. Meanwhile, Liu, et al. consider the piecewise-quadratic FE discretization to improve the spatial convergence rate. The efficient implementation based on fast Toeplitz-matrix multiplications [48–50] of their proposed scheme is also reported. For space-time nonlocal diffusion equations, Chen, et al. [47] propose a numerical scheme, by exploiting the quadrature-based FD method in time and the Fourier spectral method in space, and show its stability. Moreover, it is shown that the convergence is uniform at a rate of $\mathcal{O}(\delta + \sigma^2)$ (where δ and σ are the time and space horizon parameters) under certain regularity assumptions on initial and source data. Even these are several methods with linear solvers of quasilinear complexity, the implementation of the above methods is still complicated, especially the computation of entries of stiffness matrix in FE discretization or finding the modes in terms of expansion basis in spectral method, cf. [26, 43, 46, 47]. In particular, it is pointed out that “More than 95% of CPU time is used to assembly routine” for their FE methods [42].

On the other hand, most of the above mentioned methods overlook that the presence of the kernel $(t - s)^{-\gamma}$ produces solutions of Eq. (1.1) with a weak singularity at $t = 0$, so that approximation methods (e.g., $L1$ formula) on *uniform meshes* have a poor convergent rate and high computational cost [47, 51–53]. In this work, we contribute to developing fast implicit difference schemes (IDSs) for solving the TSFDE (1.1), the direct scheme utilizes the simple FD discretization [37] and the graded $L1$ formula [52] for approximating the IFL and the Caputo fractional derivative, where the non-uniform temporal discretization can overcome the initial singularity. Due to the repeat summation of numerical solutions in the previous steps, the direct scheme always needs much CPU time and memory cost, especially for the larger number of time steps. In order to alleviate the computational cost, the sum-of-exponential (SOE) approximation [54] of the kernel $(t - s)^{-\gamma}$ in the graded $L1$ formula for Caputo fractional derivative can be efficiently evaluated via the recurrence method. Thus, we can derive the fast implicit difference scheme. In particular, we revisit the matrix properties of the discretized IFL and prove the discretized matrix is a strictly diagonal dominant and symmetric M -matrix with positive diagonal elements (i.e., the symmetric positive definite matrix), which is not studied in [37]. Based on such matrix properties, we strictly prove that the fast numerical schemes for the TSFDE (1.1) are unconditionally stable and present the corresponding error estimates of $\mathcal{O}(M^{-\min\{r\gamma, 2-\gamma\}} + h^2)$ (h is the spatial grid size) under certain regularity assumptions on the smooth solutions. To our best knowledge, there are few successful attempts to derive the efficient IDSs for solving the TSFDE (1.1) with strict theoretical analyses. This is one of main attractive advantages of our proposed methods compared to the above mentioned methods.

In addition, the nonlocality of IFL results in the dense discretized linear systems, which is the leading time-consuming part in practical implementations [26, 42, 43]. Fortunately, the coefficient matrix of discretized linear systems enjoys the Toeplitz-like structure [37–39], it means that we solve the sequence of discretized linear systems in a matrix-free pattern [29, 50, 55], because the Toeplitz matrix-vector products can be computed via fast Fourier transforms (FFTs) in $\mathcal{O}(N \log N)$ operations. More precisely, we will adopt the circulant preconditioners [48–50] for accelerating the Krylov subspace solvers [49] for the sequence of

discretized linear systems. Moreover, the benefit of circulant preconditioners will be verified via both theoretical and numerical results. It notes that fast schemes greatly reduce the computational work of solving the discretized linear systems from $\mathcal{O}(MN^3 + M^2N)$ by a direct solver to $\mathcal{O}(MN(\log N + N_{exp}))$ per preconditioned Krylov subspace iteration and a memory requirement from $\mathcal{O}(MN^2)$ to $\mathcal{O}(NN_{exp})$ (cf. Section 2 for defining N_{exp}).

The contributions of the current work can be summarized as follows.

- We present two IDSs for solving the TSFDE (1.1) with non-smooth data and these numerical schemes can be easily extended to solve the multi-dimensional cases.
- Both the stability and convergence analysis of these IDSs can be strictly proved via the discretized matrix properties.
- We provide the efficient implementation with theoretical guarantee of the fast IDSs for reducing the computation and memory cost deeply.

The rest of this paper is organized as follows. In Section 2, we review some information about the spatial and temporal discretizations and truncated error analyses. In Section 3, both direct and fast IDSs are derived for the TSFDE (1.1), then their stability and convergence are also proved by revisiting the properties of spatial discretized matrix. In Section 4, the efficient implementation based on fast preconditioned Krylov subspace solvers of the proposed IDSs are given and the accelerating benefit of circulant preconditioners is theoretical guaranteed by the clustering eigenvalues around 1. Section 5 presents numerical results to support our theoretical findings and the effectiveness of the proposed IDSs. Finally, the paper closes with conclusions in Section 6.

2. Preliminaries

In this section we present necessary definitions and auxiliary results concerning the approximations of Caputo fractional derivative and fractional Laplacian, respectively. Since we are going to develop the numerical schemes for solving Eq. (1.1), here we assume that the problem (1.1) has a solution $u(x, t)$, such that

$$\left| \frac{\partial^k u(x, t)}{\partial t^k} \right| \leq c_0 t^{\gamma-k}, \quad 0 \leq k \leq 3, \quad (2.1)$$

here and in what follows, \hat{C} and c_j ($j = 0, 1, 2$) are positive constants, which depend on the problem but not on the mesh parameters [52]. Let $M, N, r \in \mathbb{N}^+$ (positive integers), $h = 2l/N$, $x_i = -l + ih$, $t_m = (m/M)^r T$ and $\tau_m = t_m - t_{m-1}$. We also consider the sets

$$\Omega_h = \{x_i | 0 \leq i \leq N\}, \quad \Omega_\tau = \{t_m | 0 \leq m \leq M\}, \quad \Omega_{h,\tau} = \{(x_i, t_m) | 0 \leq i \leq N, 0 \leq m \leq M\}$$

and let $v = \{v_i^m | 0 \leq i \leq N, 0 \leq m \leq M\}$ be a grid function on $\Omega_{h,\tau}$. We consider the set $\mathcal{V}_h = \{\mathbf{v} | \mathbf{v} = (v_0, v_1, \dots, v_{N-1}, v_N)\}$ of grid functions on Ω_h and provide it with the norm

$$\|\mathbf{v}\|_\infty = \max_{0 \leq i \leq N} |v_i|.$$

Then, the following lemma introduced in [52] provides a complete description of the discretization of Caputo fractional derivative at the point t_m .

Lemma 2.1. *If $|u''(t)| \leq c_0 t^{\gamma-2}$, $0 \leq t \leq T$, then there exists $\hat{C} > 0$ such that*

$$|{}_0^C D_t^\gamma u(t_m) - D_t^\gamma u(t_m)| \leq \hat{C} m^{-\min\{r(1+\gamma), 2-\gamma\}}, \quad m = 1, 2, \dots, M, \quad (2.2)$$

where $D_t^\gamma u(t_m) = \frac{1}{\Gamma(1-\gamma)} \left[a_m^{(m,\gamma)} u(t_m) - \sum_{k=1}^{m-1} (a_{k+1}^{(m,\gamma)} - a_k^{(m,\gamma)}) u(t_k) a_1^{(m,\gamma)} u(t_0) \right]$ and

$$a_k^{(m,\gamma)} = \frac{1}{\tau_k} \int_{t_{k-1}}^{t_k} \frac{ds}{(t_m - s)^\gamma}. \quad (2.3)$$

Meanwhile, further properties of the coefficients $a_k^{(m,\gamma)}$ can be found in [52, Lemma 2.2]. On the other hand, it notes that using Lemma 2.1 in practical applications always needs much computational cost due to evaluating the sums of the solutions of previous time steps repeatedly. In order to reduce the cost, here it is meaningful to develop the fast numerical approximation of Caputo fractional derivative on a non-uniform temporal mesh.

Lemma 2.2. ([54]) *Let ϵ denote the tolerance error, δ cut-off time restriction and T final time. Then there exist an $N_{exp} \in \mathbb{N}^+$ and $s_j, w_j > 0$, $j = 1, 2, \dots, N_{exp}$ such that*

$$\left| t^{-\gamma} - \sum_{j=1}^{N_{exp}} w_j e^{-s_j t} \right| \leq \epsilon, \quad \text{for any } t \in [\delta, T],$$

where $N_{exp} = \mathcal{O}((\log \epsilon^{-1})(\log \log \epsilon^{-1} + \log(T\delta^{-1})) + (\log \delta^{-1})(\log \log \epsilon^{-1} + \log \delta^{-1}))$.

Based on Lemma 2.2, we set $\delta = (1/M)^r T$ and then the fast algorithm for computing Caputo fractional derivative on a graded temporal grid can be drawn as follows.

Lemma 2.3. *If $|u'(t)| \leq c_0 t^{\gamma-1}$ and $|u''(t)| \leq c_0 t^{\gamma-2}$, then*

$${}_0^C D_t^\gamma u(t_m) = {}^{FC} D_t^\gamma u(t_m) + \mathcal{O}(m^{-\min\{r(1+\gamma), 2-\gamma\}} + \epsilon), \quad m = 1, 2, \dots, M, \quad (2.4)$$

where ${}^{FC} D_t^\gamma u(t_m) = \frac{1}{\Gamma(1-\gamma)} \left[b_m^{(m,\gamma)} u(t_m) - \sum_{k=1}^{m-1} (b_{k+1}^{(m,\gamma)} - b_k^{(m,\gamma)}) u(t_k) - b_1^{(m,\gamma)} u(t_0) \right]$ with

$$b_k^{(m,\gamma)} = \begin{cases} \sum_{j=1}^{N_{exp}} w_j \frac{1}{\tau_k} \int_{t_{k-1}}^{t_k} e^{-s_j(t_m-s)} ds, & k = 1, 2, \dots, m-1, \\ a_m^{(m,\gamma)}, & k = m. \end{cases} \quad (2.5)$$

Similarly, the properties of the coefficients $\{b_k^{(m,\gamma)}\}$ can be found in [52, Lemma 2.4]. Moreover, we should provide the information for approximating the (regional) IFL. According to the idea in [37], we first introduce the notations

$$\begin{aligned}
(-\Delta)_{h,\mu}^{\alpha/2} u(x_i) = & C_{\alpha,\mu}^h \left[\left(\sum_{\ell=2}^{N-1} \frac{(\ell+1)^\nu - (\ell-1)^\nu}{\ell^\mu} + \frac{N^\nu - (N-1)^\nu}{N^\mu} + (2^\nu + \kappa_\mu - 1) \right. \right. \\
& + \left. \frac{2\nu}{\alpha N^\alpha} \right) u(x_i) - \frac{2^\nu + \kappa_\mu - 1}{2} (u(x_{i-1}) + u(x_{i+1})) \\
& \left. - \frac{1}{2} \sum_{j=1, j \neq i, i \pm 1}^{N-1} \frac{(|j-i|+1)^\nu - (|j-i|-1)^\nu}{|j-i|^\mu} u(x_j) \right], \tag{2.6}
\end{aligned}$$

where $i = 1, 2, \dots, N-1$, $C_{\alpha,\mu}^h = c_{1,\alpha}/(\nu h^\alpha) > 0$ and the constant $\kappa_\mu = 1$ for $\mu \in (\alpha, 2)$, while $\kappa_\mu = 2$ if $\mu = 2$. Meanwhile, we denote $\nu = \mu - \alpha$ for notational simplicity.

Lemma 2.4. ([37]) *Suppose that $u(x) \in \mathcal{C}^{s, \frac{s}{2}}(\mathbb{R})$ has the finite support on an open set $\Omega \subset \mathbb{R}$, and defined in (2.6) is a finite difference approximation of the fractional Laplacian $(-\Delta)^{\alpha/2}$. Then, for any $\mu \in (\alpha, 2)$, there is*

$$\|(-\Delta)^{\alpha/2} u(x) - (-\Delta)_{h,\mu}^{\alpha/2} u(x)\|_{\infty, \Omega} \leq \tilde{C} h^p \tag{2.7}$$

with $\tilde{C} > 0$ depending on α and μ . Here $p \in (0, 2]$ would be determined via the regularity (i.e., the index $s \in \mathbb{N}$) of $u(x)$.

Lemma 2.4 provide a direct discretization for the IFL appeared in the TSFDE (1.1). At present, the spatial and temporal discretizations are ready for studying the numerical methods, which will be described in the next section.

3. Direct and fast implicit difference schemes

In this section, we will establish two implicit difference schemes for solving the problem (1.1). Meanwhile, the stability, convergence and error analysis of such difference schemes are investigated and proved in details.

3.1. Two implicit difference schemes

Let us introduce the fast difference schemes for solving the problem (1.1). Evaluating the Eq. (1.1) at the points (x_i, t_m) , we have

$${}_0^C D_t^\gamma u(x_i, t_m) = -\kappa(x_i, t_m) (-\Delta)^{\alpha/2} u(x_i, t_m) + f(x_i, t_m), \tag{3.1}$$

where $1 \leq i \leq N-1, 1 \leq m \leq M$. Let U be a grid function defined by

$$U_i^m := u(x_i, t_m), \quad f_m^i = f(x_i, t_m), \quad \kappa_i^m = \kappa(x_i, t_m), \quad 0 \leq i \leq N, 0 \leq m \leq M.$$

Using this notation and recalling Lemma 2.3 along with Lemma 2.4, we can write Eq. (1.1) at grid point (x_i, t_m) as follows

$$\begin{cases}
{}_0^{FC} D_t^\gamma U_i^m = -\kappa_i^m (-\Delta)_{h,\mu}^{\alpha/2} U_i^m + f_m^i + R_i^m, & 1 \leq i \leq N-1, 1 \leq m \leq M, \\
U_0^m = U_N^m \equiv 0, & 0 \leq m \leq M, \\
U_i^0 = \phi(x_i), & 1 \leq i \leq N-1,
\end{cases} \tag{3.2}$$

of $(-\Delta)^{\alpha/2}u(x, t)$ can be expressed in the matrix-vector product form $(-\Delta)_{h,\mu}^{\alpha/2}\mathbf{u}^m = A\mathbf{u}^m$, where $A = [a_{ij}]_{i,j=1,\dots,N-1}$ is the matrix representation of the (discretized) fractional Laplacian, defined as

$$a_{ij} = C_{\alpha,\mu}^h \begin{cases} \sum_{\ell=2}^{N-1} \frac{(\ell+1)^\nu - (\ell-1)^\nu}{\ell^\mu} + \frac{N^\nu - (N-1)^\nu}{N^\mu} + (2^\nu + \kappa_\mu - 1) + \frac{2\nu}{\alpha N^\alpha}, & j = i, \\ -\frac{2^\nu + \kappa_\mu - 1}{2}, & j = i \pm 1, \\ -\frac{(|j-i|+1)^\nu - (|j-i|-1)^\nu}{2|j-i|^\mu}, & j \neq i, i \pm 1, \end{cases} \quad (3.6)$$

where $i, j = 1, 2, \dots, N-1$. It is easy to see that the matrix A is a real symmetric Toeplitz matrix, which can be stored with only $(N-1)$ entries [37, 48, 49]. Moreover, we can give the following conclusions:

Proposition 3.1. *According to the definition of A , it holds*

- 1) A is a strictly diagonally dominant M -matrix;
- 2) A is symmetric positive definite;
- 3) The decay in absolute values of the entries A_{ij} along the diagonals, i.e., $a_{11} > |a_{12}| > \dots > |a_{1,N-1}|$ and $\lim_{N \rightarrow \infty} |a_{1,N-1}| = 0$.

Proof. 1) Since A is a symmetric Toeplitz matrix, then the diagonal entries are equal to $a_{11} > 0$ – cf. Eq. (3.6). Moreover, it is not hard to see that $a_{ij} < 0$ ($i \neq j$). So it concludes that A is an M -matrix [56, p. 533] and we use the definition of $A \in \mathbb{R}^{(N-1) \times (N-1)}$ to consider

$$\begin{aligned} a_{11} - \sum_{j \neq 1} |a_{1j}| &= a_{11} - \sum_{j=2}^{N-1} |a_{1j}| \\ &> C_{\alpha,\mu}^h \left[\frac{2^\nu + \kappa_\mu - 1}{2} + \frac{N^\nu - (N-1)^\nu}{N^\mu} + \frac{2\nu}{\alpha N^\alpha} \right] > 0. \end{aligned} \quad (3.7)$$

and

$$a_{N-1,N-1} - \sum_{j \neq N-1} |a_{N-1,j}| = a_{11} - \sum_{j=2}^{N-1} |a_{1j}| > 0. \quad (3.8)$$

Similarly, it follows that

$$\begin{aligned} a_{ii} - \sum_{j \neq i} |a_{ij}| &= a_{11} - \sum_{j \neq i} a_{ij} \\ &> C_{\alpha,\mu}^h \left[\frac{N^\nu - (N-1)^\nu}{N^\mu} + \frac{2\nu}{\alpha N^\alpha} \right] > 0, \quad i = 2, 3, \dots, N-2, \end{aligned} \quad (3.9)$$

a combination of the aforementioned three inequalities verifies that A is a strictly diagonally dominant M -matrix;

2) Since A is a symmetric strictly diagonally dominant M -matrix and all its diagonal elements are positive, i.e., $a_{ii} = a_{11} > 0$, thus A is indeed a symmetric positive definite matrix [56, Corollary 7.2.3];

3) First of all, we rewrite the matrix $A = C_{\alpha,\mu}^h \tilde{A} = C_{\alpha,\mu}^h [\tilde{a}_{ij}]_{i,j=1,\dots,N-1}$ -cf. Eq. (3.6). Meanwhile, it is easy to note that $a_{11} > |a_{12}|$, then we find

$$\begin{aligned} |\tilde{a}_{12}| - |\tilde{a}_{13}| &= \frac{2^\nu + \kappa_\mu - 1}{2} - \frac{3^\nu - 1}{2^{\mu+1}} \\ &\geq \frac{4^{\nu+\alpha/2} - 3^\nu + 1}{2^{\nu+\alpha+1}} > 0. \end{aligned} \quad (3.10)$$

For $j = 3, 4, \dots$, we set $|j - i| = |j - 1| = k$, thus $k \geq 2$ and

$$\begin{aligned} |\tilde{a}_{1j}| &:= f(k) = \frac{k^{-\alpha}}{2} \cdot \left[\left(1 + \frac{1}{k}\right)^\nu - \left(1 - \frac{1}{k}\right)^\nu \right] \\ &= \left[\binom{\nu}{1} k^{-1-\alpha} + \binom{\nu}{3} k^{-3-\alpha} + \binom{\nu}{5} k^{-5-\alpha} + \dots \right] \\ &\sim \mathcal{O}(k^{-1-\alpha}), \end{aligned} \quad (3.11)$$

which should implies that $f(k) > f(k+1)$. Therefore, it follows that $a_{11} > |a_{12}| > \dots > |a_{1,N-1}|$. \square

According to Proposition 3.1, if we define

$$\mathcal{D}(C) = \min_{1 \leq i \leq N-1} \left(|C_{ii}| - \sum_{1 \leq j \leq N-1, j \neq i} |C_{ij}| \right) \quad (3.12)$$

for any matrix $C = [C_{ij}]_{i,j=1,\dots,N-1}$, then it follows that $\mathcal{D}(A) \geq 0$, which is helpful in the next context. The following properties of the operator $\mathcal{D}(\cdot)$ can be given as follows,

Lemma 3.1. ([57, Lemma 3]) *Let $C_1, C_2 \in \mathbb{R}^{(N-1) \times (N-1)}$. Suppose both C_1 and C_2 have positive diagonal entries, then it follows that $\mathcal{D}(C_1 + C_2) \geq \mathcal{D}(C_1) + \mathcal{D}(C_2)$.*

Lemma 3.2. ([57, Lemma 4]) *Let $C \in \mathbb{R}^{(N-1) \times (N-1)}$. Suppose $\mathcal{D}(C) \geq 0$. Then for any nonnegative diagonal matrix $K \in \mathbb{R}^{(N-1) \times (N-1)}$, it holds $\mathcal{D}(KC) \geq \mathcal{D}(C) \min_{1 \leq j \leq N-1} K_{jj} \geq 0$.*

Next, we exploit the above two lemmas to give the following estimation about the coefficient matrices $\mathcal{M}^{(m)}$ of Eq. (3.5).

Theorem 3.1. *For any $\frac{b_m^{(m,\gamma)}}{\Gamma(1-\gamma)} > 0$ and $1 \leq m \leq M$, it holds $\min_{1 \leq m \leq M} \mathcal{D}\left(\frac{1}{\Gamma(1-\gamma)} b_m^{(m,\gamma)} I + K^{(m)} A\right) \geq \frac{b_m^{(m,\gamma)}}{\Gamma(1-\gamma)}$.*

Proof. From Lemmas 3.1–3.2 and Proposition 3.1, we obtain

$$\begin{aligned} \mathcal{D}\left(\frac{1}{\Gamma(1-\gamma)} b_m^{(m,\gamma)} I + K^{(m)} A\right) &\geq \mathcal{D}\left(\frac{1}{\Gamma(1-\gamma)} b_m^{(m,\gamma)} I\right) + \mathcal{D}(K^{(m)} A) \\ &\geq \frac{b_m^{(m,\gamma)}}{\Gamma(1-\gamma)}, \quad 1 \leq m \leq M, \end{aligned} \quad (3.13)$$

from which the result follows. \square

Before proving the final result of this section on the unconditional stability and convergence property of the FIDS (3.3), we still need to recall the following useful lemma.

Lemma 3.3. *Suppose $C \in \mathbb{R}^{(N-1) \times (N-1)}$ satisfies $\mathcal{D}(C) \geq \lambda > 0$. Then, for any $\mathbf{y} \in \mathbb{R}^{N-1}$, it holds $\lambda \|\mathbf{y}\|_\infty \leq \|C\mathbf{y}\|_\infty$.*

Proof. Since $\mathcal{D}(C) \geq \lambda > 0$, then $\mathcal{D}(\frac{1}{\lambda}C) \geq 1$ and $\|\mathbf{y}\|_\infty \leq \|\frac{C}{\lambda}\mathbf{y}\|_\infty$ [57, Lemma 7], which proves the above result. \square

Theorem 3.2. *The proposed FIDS (3.3) with $\epsilon \leq c_1 M^\gamma$ is uniquely solvable and unconditionally stable in the sense that*

$$\|\mathbf{u}^k\|_\infty \leq \|\mathbf{u}^0\|_\infty + \Gamma(1 - \gamma) \max_{1 \leq s \leq k} \frac{\|\mathbf{f}^s\|_\infty}{b_1^{(s,\gamma)}}, \quad k = 1, 2, \dots, M, \quad (3.14)$$

where $\|\mathbf{f}^s\|_\infty \leq \max_{1 \leq i \leq N-1} |f_i^s|$.

Proof. In order to the unique solvability is equivalent to show the invertibility of $\mathcal{M}^{(m)}$ for each $1 \leq m \leq M$. By means of Theorem 3.1 and Lemma 3.3, it follows that

$$\|\mathcal{M}^{(m)}\mathbf{y}\|_\infty = \left\| \left[\frac{1}{\Gamma(1 - \gamma)} b_m^{(m,\gamma)} I + K^{(m)} A \right] \mathbf{y} \right\|_\infty \geq \frac{b_m^{(m,\gamma)}}{\Gamma(1 - \gamma)} \|\mathbf{y}\|_\infty, \quad \forall \mathbf{y} \in \mathbb{R}^{N-1}, \quad (3.15)$$

where $1 \leq m \leq M$. Therefore, $\mathcal{M}^{(m)} : \mathbb{R}^{N-1} \mapsto \mathbb{R}^{N-1}$ is clearly an injection for each $1 \leq m \leq M$, whose null space is simply $\{\mathbf{0}\}$. Hence, $\mathcal{M}^{(m)}$'s are nonsingular, which proves the unique solvability.

On the other hand, we apply Eq. (3.15) and the monotonicity of $\{b_k^{(m,\gamma)}\}$ ($1 \leq m \leq M$) [52, Lemma 2.4] to obtain

$$b_m^{(m,\gamma)} \|\mathbf{u}^m\|_\infty \leq \sum_{k=1}^{m-1} (b_{k+1}^{(m,\gamma)} - b_k^{(m,\gamma)}) \|\mathbf{u}^k\|_\infty + b_1^{(m,\gamma)} \left[\|\mathbf{u}^0\|_\infty + \frac{\Gamma(1 - \gamma)}{b_1^{(m,\gamma)}} \|\mathbf{f}^m\|_\infty \right], \quad 1 \leq m \leq M.$$

Then the inequality (3.14) can be proved by the method of mathematical induction, which is similar to the proof of [52, Theorem 4.1], we omit the details here. \square

On the other hand, we replace the coefficients $\{b_k^{(m,\gamma)}\}$ with $\{a_k^{(m,\gamma)}\}$ in Theorem 3.1, Eqs. (3.5) and (3.15), then we can obtain the following conclusion, which is helpful to analyze the stability and convergence of DIDS (3.4).

Theorem 3.3. *The proposed DIDS (3.4) is uniquely solvable and unconditionally stable in the sense that*

$$\|\mathbf{u}^k\|_\infty \leq \|\mathbf{u}^0\|_\infty + \Gamma(1 - \gamma) \max_{1 \leq s \leq k} \frac{\|\mathbf{f}^s\|_\infty}{a_1^{(s,\gamma)}}, \quad k = 1, 2, \dots, M. \quad (3.16)$$

Proof. The proof of this theorem is similar to Theorem 3.3, we omit the details here. \square

From Theorems 3.1–3.3, we may see that both FIDS (3.3) and DIDS (3.4) are stable to the initial value ϕ and the right hand term f . Now, we consider the convergence of these two difference schemes.

Theorem 3.4. *Let $\{U_i^m | 0 \leq i \leq N, 0 \leq m \leq M\}$ and $\{u_i^m | 0 \leq i \leq N, 0 \leq m \leq M\}$ be, respectively, the solutions of the problem (1.1) and the difference scheme (3.3). If $\epsilon \leq \min\{c_1 M^\gamma, T^{-\gamma/2}\}$, then*

$$\|e^m\|_\infty \leq 2\Gamma(1-\gamma)c_2 T^\gamma (M^{-\min\{r\gamma, 2-\gamma\}} + h^p + \epsilon), \quad 1 \leq m \leq M, \quad (3.17)$$

where $e_i^m = U_i^m - u_i^m$, $0 \leq i \leq M$, $0 \leq m \leq M$ and p would be determined via the spatial regularity of $u(x, t)$.

Proof. Writing the system (3.2) as

$$\begin{cases} \frac{1}{\Gamma(1-\gamma)} \left[b_m^{(m,\gamma)} U_i^m - \sum_{k=1}^{m-1} (b_{k+1}^{(m,\gamma)} - b_k^{(m,\gamma)}) U_i^k - b_1^{(m,\gamma)} U_i^0 \right] = -\kappa(-\Delta)_{h,\mu}^{\alpha/2} U_i^m \\ \quad \quad \quad \quad \quad \quad \quad \quad \quad \quad \quad \quad \quad \quad \quad + f_i^m + R_i^m, & 1 \leq i \leq N-1, 1 \leq m \leq M, \\ U_0^m = U_N^m = 0, & 0 \leq m \leq M, \\ U_i^0 = \phi(x_i), & 1 \leq i \leq N-1, \end{cases}$$

and subtracting the Eq. (3.3) from the corresponding above system

$$\begin{cases} \frac{1}{\Gamma(1-\gamma)} \left[b_m^{(m,\gamma)} e_i^m - \sum_{k=1}^{m-1} (b_{k+1}^{(m,\gamma)} - b_k^{(m,\gamma)}) e_i^k - b_1^{(m,\gamma)} e_i^0 \right] = -\kappa(-\Delta)_{h,\mu}^{\alpha/2} e_i^m \\ \quad \quad \quad \quad \quad \quad \quad \quad \quad \quad \quad \quad \quad \quad \quad + R_i^m, & 1 \leq i \leq N-1, 1 \leq m \leq M, \\ e_0^m = e_N^m = 0, & 0 \leq m \leq M, \\ e_i^0 = 0, & 1 \leq i \leq N-1, \end{cases} \quad (3.18)$$

By means of Theorem 3.1 and the matrix analysis described above, it follows that

$$\|e^m\|_\infty \leq \Gamma(1-\gamma) \max_{1 \leq s \leq m} \frac{\|f^s\|_\infty}{b_1^{(s,\gamma)}}, \quad m = 1, 2, \dots, M,$$

the rest of this proof is also similar to [52, Theorem 4.2].

Again, we employ the similar strategy to give the error analysis of DIDS (3.4) as follows.

Theorem 3.5. *Let $\{U_i^m | 0 \leq i \leq N, 0 \leq m \leq M\}$ and $\{u_i^m | 0 \leq i \leq N, 0 \leq m \leq M\}$ be, respectively, the solutions of the problem (1.1) and the difference scheme (3.4), then*

$$\|e^m\|_\infty \leq \mathcal{O}(M^{-\min\{r\gamma, 2-\gamma\}} + h^p), \quad 1 \leq m \leq M, \quad (3.19)$$

where $e_i^m = U_i^m - u_i^m$, $0 \leq i \leq M$, $0 \leq m \leq M$.

In practice, the value of ϵ is sufficiently fixed such that the tolerance error in (3.17) can be negligible as compared with the space and time errors. Then it also finds that the numerical errors for DIDS and FIDS are almost identical but the later is often faster – cf. Section 5. With the help of arguments in proving [37, Theorems 3.1-3.2], it is not hard to make the above convergence results described in Theorems 3.4–3.5 more specific.

Remark 3.1. *For determining the value of p , it reads*

- *Suppose that the solution of the problem (1.1) satisfies the condition (2.1) and $u(x, \cdot) \in \mathcal{C}^{s, \alpha/2}(\mathbb{R})$ with $(x, t) \in \mathbb{R} \times [0, T]$ and $s \geq 1$, then solutions of FIDS (3.3) and DIDS (3.4) with $\mu \in (\alpha, 2)$ converge to the exact solutions of Eq. (1.1), respectively;*
- *For $s = 1$, $\alpha \in (0, 2)$ and $\mu \in (\alpha, 2]$, the convergence rates of FIDS (3.3) and DIDS (3.4) are (at least) $\mathcal{O}(M^{-\min\{r\gamma, 2-\gamma\}} + h^{1-\frac{\alpha}{2}})$ and $\mathcal{O}(M^{-\min\{r\gamma, 2-\gamma\}} + h^{1-\frac{\alpha}{2}} + \epsilon)$, respectively; see [37, 38] for details.*
- *For $s \geq 3$ and $\alpha \in (0, 2)$, the convergence rates of FIDS (3.3) and DIDS (3.4) with $\mu = 2$ or $\mu = 1 + \alpha/2$ are $\mathcal{O}(M^{-\min\{r\gamma, 2-\gamma\}} + h^2)$ and $\mathcal{O}(M^{-\min\{r\gamma, 2-\gamma\}} + h^2 + \epsilon)$, respectively.*

Moreover, we will work out some numerical results for supporting the above theoretical convergence behaviors in Section 5.

4. Efficient implementation based on preconditioning of the difference schemes

In the section, we analyze both the implementation and computational complexity of FIDS (3.3) and DIDS (3.4) and we propose an efficient implementation utilized preconditioned Krylov subspace solvers. Noting that $a_m^{(m, \gamma)} = b_m^{(m, \gamma)} > 0$, we start the efficient implementation from the following matrix form of these two implicit difference schemes at the time level $1 \leq m \leq M$, which are given by Eq. (3.5) and

$$\mathcal{M}^{(m)} \mathbf{u}^m = \frac{1}{\Gamma(1-\gamma)} \left[\sum_{k=1}^{m-1} (a_{k+1}^{(m, \gamma)} - a_k^{(m, \gamma)}) \mathbf{u}^k - a_1^{(m, \gamma)} \mathbf{u}^0 \right] + \mathbf{f}^m, \quad (4.1)$$

respectively. From Theorems 3.2-3.3, it knows that both Eq. (3.5) and Eq. (4.1) have the unique solutions. In addition, it is meaningful to remark that Eq. (3.5) and Eq. (4.1) corresponding to FIDS (3.3) and DIDS (3.4) are inherently sequential, thus they are both difficult to parallelize over time.

4.1. The circulant preconditioner

On the other hand, it is useful to note that the matrix-vector product $\mathcal{M}^{(m)} \mathbf{v}$ can be efficiently calculated by

$$\mathcal{M}^{(m)} \mathbf{v} = \frac{1}{\Gamma(1-\gamma)} b_m^{(m, \gamma)} \mathbf{v} + K^{(m)}(A\mathbf{v}), \quad (4.2)$$

where $\mathbf{v} \in \mathbb{R}^{N-1}$ is any vector and the Toeplitz matrix-vector $A\mathbf{v}$ can be implicitly evaluated via the FFTs in $\mathcal{O}(N \log N)$ operations. In other words, we can use a *matrix-free* method to compute $\mathcal{M}^{(m)} \mathbf{v}$ quickly. Based on such observations, the Krylov subspace method should be

the most suitable solver for Eq. 3.5 or Eq. (4.1) one by one. However, when the coefficients and the order of integral fractional Laplacian are not small, then the coefficient matrices $\mathcal{M}^{(m)}$ will be increasingly ill-conditioned (cf. Section 5). This fact deeply slows up the convergence of the Krylov subspace method, while the preconditioning techniques are often used to overcome this difficulty [29, 48–50]. In the literature on Toeplitz systems, circulant preconditioners always played important roles [48, 49]. In fact, circulant preconditioners have been theoretically and numerically studied with applications to fractional partial differential equations for recent years; see for instances [29, 39, 50].

In this work, we design a family of the Strang’s preconditioners [48] for accelerating the convergence of Krylov subspace solvers. More precisely, the circulant preconditioners are given for Eq. 3.5 and/or Eq. (4.1) as follows,

$$\mathcal{P}^{(m)} = \frac{1}{\Gamma(1-\gamma)} b_m^{(m,\gamma)} I + \kappa^{(m)} s(A) = F^* \left[\frac{1}{\Gamma(1-\gamma)} b_m^{(m,\gamma)} + \kappa^{(m)} \Lambda \right] F, \quad (4.3)$$

where F and F^* are the Fourier matrix and its conjugate transpose, respectively, and the scalar $\kappa^{(m)} = \frac{1}{N-1} \sum_{i=1}^{N-1} \kappa_i^m$. Meanwhile, $s(A) = F^* \Lambda F$ is the Strang circulant approximation [48, 49] of the Toeplitz matrix A and the diagonal matrix Λ contains all the eigenvalues of $s(A)$ with the first column: $\mathbf{c}_S = [a_{11}, \dots, a_{1, \lfloor \frac{N+1}{2} \rfloor}, a_{1, \lfloor \frac{N}{2} \rfloor}, \dots, a_{12}]^\top \in \mathbb{R}^{N-1}$. Therefore the matrix $\Lambda = \text{diag}(F \mathbf{c}_S)$ can be *computed in advance and only one time during each time level*. Besides, as $\mathcal{P}^{(m)}$ are the circulant matrices, we observe from Eq. (4.3) that the inverse-matrix-vector product $\mathbf{z} = [\mathcal{P}^{(m)}]^{-1} \mathbf{v}$ can be carried out in $\mathcal{O}(N \log N)$ operations via the (inverse) FFTs. In one word, we exploit a fast preconditioned Krylov subspace method with only $\mathcal{O}(N)$ memory requirement and $\mathcal{O}(N \log N)$ computational cost per iteration, while the number of iterations and the computational cost are greatly reduced.

To investigate the properties of the proposed preconditioners, the following lemma is the key to prove the invertibility of $\mathcal{P}^{(m)}$ in Eq. (4.3).

Lemma 4.1. *All eigenvalues of $s(A)$ fall inside the open disc*

$$\{z \in \mathbb{R} : |z - a_{11}| < a_{11}\}, \quad (4.4)$$

and all the eigenvalues of $s(A)$ are strictly positive for all N .

Proof. First of all, since the matrix A is symmetric, then $s(A)$ is also symmetric and its eigenvalues should be real. All the Gershgorin disc of the circulant matrix $s(A)$ are centered at a_{11} with radius

$$r_N = 2 \sum_{\ell=2}^{\lfloor \frac{N+1}{2} \rfloor} |a_{1,\ell}| < a_{11}, \quad (4.5)$$

the above inequality holds due to the expression of Eq. (3.6), where the expression of a_{11} contains exactly the sum of $2|a_{1,\ell}|$ ($\ell = 2, 3, \dots, N-1$). In conclusion, all the eigenvalues of $s(A)$ are strictly positive for all N . \square

According to Lemma 4.1, it means that $s(A)$ is a real symmetric positive definite matrix. Moreover, the invertibility of circulant preconditioners $\mathcal{P}^{(m)}$ (4.3) can be given for all $m = 1, 2, \dots, M$ as follows.

Lemma 4.2. *Let $\alpha \in (0, 2)$. The preconditioner $\mathcal{P}^{(m)}$ is invertible and*

$$\left\| (\mathcal{P}^{(m)})^{-1} \right\|_2 < \frac{1}{\frac{b_m^{(m,\gamma)}}{\Gamma(1-\gamma)} + \kappa^{(m)} \cdot \min_{1 \leq k \leq N-1} [\Lambda]_{k,k}}, \quad (4.6)$$

Proof. According to Lemma 4.1, we have $[\Lambda]_{k,k} > 0$. Noting that $a_m^{(m,\gamma)} > 0$ (or $b_m^{(m,\gamma)} > 0$) and $\kappa^{(m)} > 0$, we have

$$\left[\frac{1}{\Gamma(1-\gamma)} b_m^{(m,\gamma)} + \kappa^{(m)} \Lambda \right]_{k,k} > 0 \quad (4.7)$$

for $k = 1, 2, \dots, N-1$. Therefore, $\mathcal{P}^{(m)}$ is invertible. Furthermore, we have

$$\left\| (\mathcal{P}^{(m)})^{-1} \right\|_2 = \frac{1}{\min_{1 \leq k \leq N-1} \left[\frac{1}{\Gamma(1-\gamma)} b_m^{(m,\gamma)} + \kappa^{(m)} \Lambda \right]_{k,k}} < \frac{1}{\frac{b_m^{(m,\gamma)}}{\Gamma(1-\gamma)} + \kappa^{(m)} \cdot \min_{1 \leq k \leq N-1} [\Lambda]_{k,k}},$$

the other inequality can be similarly obtained. \square

4.2. Spectrum of the preconditioned matrix

In this subsection, we study the spectrum of the preconditioned matrix, which can help us to understand the convergence of preconditioned Krylov subspace solvers. For convenience of our investigation, we first rewrite assume that the diffusion coefficient function $\kappa(x, t) \equiv \kappa(t)$, then Eq. (3.5) or Eq. (4.1) will be a sequence of real symmetric positive definite linear systems, where the coefficient matrices reduce to $\mathcal{M}^{(m)} = \frac{1}{\Gamma(1-\gamma)} b_m^{(m,\gamma)} I + \kappa^{(m)} A$ corresponding to Eq. (3.5) and Eq. (4.1), respectively. The preconditioned CG (PCG) method [49] should be a suitable candidate for solving such linear systems one by one. Moreover, the spectrum of the preconditioned matrix $(\mathcal{P}^{(m)})^{-1} \mathcal{M}^{(m)}$ are available for both Eq. (3.5) and Eq. (4.1) at each time level m , so we take Eq. (3.5) as the research object in the next context.

Throughout this subsection, we rewrite Eq. (3.5) into the following equivalent form

$$\tilde{\mathcal{M}}^{(m)} \mathbf{u}^m = \frac{1}{\Gamma(1-\gamma) C_{\alpha,\mu}^h} \left[\sum_{k=1}^{m-1} (b_{k+1}^{(m,\gamma)} - b_k^{(m,\gamma)}) \mathbf{u}^k - b_1^{(m,\gamma)} \mathbf{u}^0 \right] + \frac{1}{C_{\alpha,\mu}^h} \mathbf{f}^m, \quad (4.8)$$

where $\tilde{\mathcal{M}}^{(m)} = \frac{b_m^{(m,\gamma)}}{\Gamma(1-\gamma) C_{\alpha,\mu}^h} I + \kappa^{(m)} \tilde{A}$ and its corresponding circulant preconditioner $\mathcal{P}^{(m)}$ reduces to $\tilde{\mathcal{P}}^{(m)} = \frac{b_m^{(m,\gamma)}}{\Gamma(1-\gamma) C_{\alpha,\mu}^h} I + \kappa^{(m)} s(\tilde{A})$, which is still invertible – cf. Lemma 4.2. Moreover, we assume that M and r are properly chosen, depending on N , such that $\eta_{N,M,r}^{(m)} \triangleq \frac{b_m^{(m,\gamma)}}{\Gamma(1-\gamma) C_{\alpha,\mu}^h}$ in (4.8) is bounded away from 0; i.e., there exist two real numbers “ $\check{\eta}$ ” and “ $\hat{\eta}$ ” such that

$$0 < \check{\eta} \leq \eta_{N,M,r}^{(m)} \leq \hat{\eta}, \quad \forall N \text{ and } m = 1, 2, \dots, M-1. \quad (4.9)$$

We add a subscript N to each matrix to denote the matrix size. Under the above assumption in (4.9), the matrix $\tilde{\mathcal{M}}^{(m)}$, $K^{(m)}$, $\eta_{N,M,r}^{(m)}$, and $\tilde{\mathcal{P}}^{(m)}$ are independent of m , and we therefore

simply denote them as $\tilde{\mathcal{M}}_{N-1}$, κ (constant), $\eta_{N,M,r}$ (constant) and $\tilde{\mathcal{P}}_{N-1}$, respectively. Now the coefficient matrix $\tilde{\mathcal{M}}^{(m)}$ in (3.5) becomes

$$\begin{aligned} \mathcal{M}_{N-1} &= \eta_{N,M,r}I + \kappa\tilde{A}_{N-1} \\ &= [\eta_{N,M,r} + \kappa(\tilde{a}_{11} - \varrho)]I + \begin{bmatrix} \varrho & \kappa\tilde{a}_{12} & \cdots & \kappa\tilde{a}_{1,N-2} & \kappa\tilde{a}_{1,N-1} \\ \kappa\tilde{a}_{12} & \varrho & \kappa\tilde{a}_{12} & \cdots & \kappa\tilde{a}_{1,N-2} \\ \vdots & \kappa\tilde{a}_{12} & \varrho & \ddots & \vdots \\ \kappa\tilde{a}_{1,N-2} & \cdots & \ddots & \ddots & \kappa\tilde{a}_{12} \\ \kappa\tilde{a}_{1,N-1} & \kappa\tilde{a}_{1,N-2} & \cdots & \kappa\tilde{a}_{12} & \varrho \end{bmatrix} \\ &\triangleq [\eta_{N,M,r} + \kappa(\tilde{a}_{11} - \varrho)]I + G_{N-1}, \end{aligned} \quad (4.10)$$

where we set $|\tilde{a}_{12}| < \varrho < \tilde{a}_{11}$ (without loss of generality), $G_{N-1} = [\tilde{g}_{ij}]_{(N-1) \times (N-1)} = [\tilde{g}_{|i-j|}]_{(N-1) \times (N-1)}$ and $\tilde{g}_{ij} = \kappa\tilde{a}_{ij}$.

To study the spectrum of the preconditioned matrix $(\mathcal{P}^{(m)})^{-1}\mathcal{M}^{(m)}$, we first introduce the *generating function* of the sequence of Toeplitz matrices $\{G_N\}_{N=1}^{\infty}$:

$$p(\theta) = \sum_{k=-\infty}^{\infty} \tilde{g}_k e^{\iota k \theta}, \quad (4.11)$$

where \tilde{g}_k is the k -th diagonal of $G_N = [\tilde{g}_{i-j}]_{N \times N}$ and $\iota = \sqrt{-1}$. The generating function $p(\theta)$ is in the *Wiener class* [48, 49] if and only if

$$\sum_{k=-\infty}^{\infty} |\tilde{g}_k| < \infty. \quad (4.12)$$

For G_{N-1} defined in (4.8), we have the following conclusion.

Lemma 4.3. *Under the above assumptions, it finds that $p(\theta)$ is real-valued and in the Wiener class.*

Proof. For convenience of our investigation, we can rewrite $p(\theta)$ for the matrix G_N defined in (4.8) as

$$p(\theta) = \tilde{g}_0 + 2 \sum_{k=1}^{\infty} \tilde{g}_k \cos(k\theta) = \varrho - 2 \sum_{k=1}^{\infty} (-\tilde{g}_k) \cos(k\theta). \quad (4.13)$$

Since it knows that $0 < -\tilde{g}_{k+1} < -\tilde{g}_k$, $\lim_{k \rightarrow \infty} (-\tilde{g}_k) = 0$ and

$$|(-\tilde{g}_k) \cos(k\theta)| < (-\tilde{g}_k)$$

with the series $\sum_{k=1}^{\infty} (-\tilde{g}_k)$ being convergent, thus the series $\sum_{k=1}^{\infty} (-\tilde{g}_k) \cos(k\theta)$ converges to a real-valued function for $\forall \theta \in [-\pi, \pi]$, which also implies that $p(\theta)$ is real-valued. According to Proposition 3.1 and its proof, it is not hard to note that $\lim_{k \rightarrow \infty} |\tilde{g}_k| = 0$. Therefore, it follows that $\sum_{k=-\infty}^{\infty} |\tilde{g}_k| < \infty$, which completes the proof. \square

In fact, Lemma 4.3 ensures the following property that the given Toeplitz matrix G_N can be approximated via a circulant matrix well.

Lemma 4.4. *If $p(\theta)$, the generating function of G_N , is in the Wiener class, then for any $\epsilon > 0$, there exist N' and $M' > 0$, such that for all $N > N'$,*

$$G_N - s(G_N) = U_N + V_N, \quad (4.14)$$

where $\text{rank}(U_N) \leq M'$ and $\|V_N\|_2 < \epsilon$.

Now we consider the spectrum of $(\tilde{\mathcal{P}}_{N-1})^{-1}\tilde{\mathcal{M}}_{N-1} - I$ is clustered around 1.

Theorem 4.1. *If $\eta_{N,M,r}$ satisfies the assumption (4.9), for any $0 < \epsilon < 1$, there exists N' and $M' > 0$ such that, for all $N > N'$, at most $2M'$ eigenvalues of the matrix $\tilde{\mathcal{M}}_{N-1} - \tilde{\mathcal{P}}_{N-1}$ have absolute values exceeding ϵ .*

Proof. With the help of Lemma 4.4, we note that

$$\begin{aligned} \tilde{\mathcal{M}}_{N-1} - \tilde{\mathcal{P}}_{N-1} &= \kappa\tilde{A} - \kappa s(\tilde{A}) \\ &= G_{N-1} - s(G_{N-1}) \\ &= U_{N-1} + V_{N-1}. \end{aligned} \quad (4.15)$$

Since both V_{N-1} and U_{N-1} are real symmetric with $\|V_{N-1}\|_2 < \epsilon$ and $\text{rank}(U_{N-1}) < M'$, hence the spectrum of V_{N-1} lies in $(-\epsilon, \epsilon)$. By the celebrated Weyl's theorem, we see that at most $2M'$ eigenvalues of $\tilde{\mathcal{M}}_{N-1} - \tilde{\mathcal{P}}_{N-1}$ have absolute values exceeding ϵ . \square

At this stage, we can see from Lemma 4.2 that

$$\|(\tilde{\mathcal{P}}_{N-1})^{-1}\|_2 = \frac{1}{\min_{1 \leq k \leq N-1} [\eta_{N,M,r} + \tilde{\Lambda}]_{k,k}} < \frac{1}{\eta_{N,M,r}} \leq \frac{1}{\tilde{\eta}}, \quad (4.16)$$

where $s(\kappa\tilde{A}) = F^*\tilde{\Lambda}F$ and the diagonal matrix $\tilde{\Lambda}$ contains all the eigenvalues of $s(\kappa\tilde{A})$. Meanwhile, we employ the fact that

$$(\tilde{\mathcal{P}}_{N-1})^{-1}\tilde{\mathcal{M}}_{N-1} - I = (\tilde{\mathcal{P}}_{N-1})^{-1}U_{N-1} - (\tilde{\mathcal{P}}_{N-1})^{-1}V_{N-1}, \quad (4.17)$$

then we have the following corollary.

Corollary 4.1. *If $\eta_{N,M,r}$ satisfies the assumption (4.9), for any $0 < \epsilon < 1$, there exists N' and $M' > 0$ such that, for all $N > N'$, at most $2M'$ eigenvalues of the matrix $(\tilde{\mathcal{P}}_{N-1})^{-1}\tilde{\mathcal{M}}_{N-1} - I$ have absolute values exceeding ϵ .*

Thus the spectrum of $(\tilde{\mathcal{P}}_{N-1})^{-1}\tilde{\mathcal{M}}_{N-1}$ is clustered around 1 for enough large N . It follows that the convergence rate of the PCG method is superlinear; refer to [48, 49] for details. Based on such observations, the preconditioner $\mathcal{P}^{(m)}$ is fairly predictable to accelerating the convergence of PCG for solving both Eq. (3.5) and Eq. (4.1) at each time level $m = 1, 2, \dots, M$ well, respectively; refer to numerical results in the next section.

Besides, although the theoretical analysis in Section 4.2 is only available for handling the model problem (1.1) with time-varying diffusion coefficients, i.e., $\kappa(x, t) \equiv \kappa(t)$, the preconditioner $\mathcal{P}^{(m)}$ is still very efficient to accelerate the convergence of nonsymmetric Krylov

subspace methods for solving Eq. (3.5) and/or Eq. (4.1) corresponding to the problem (1.1). Unfortunately, due to the variable diffusion coefficients and nonsymmetric discretized linear systems, it is still difficult to theoretically study the eigenvalue distributions of preconditioned matrices $(\mathcal{P}^{(m)})^{-1}\mathcal{M}^{(m)}$, but we still can give some figures to show the clustering eigenvalue distributions of some specified preconditioned matrices in Section 5. In summary, we can analyze the computational complexity and memory requirement for both FIDS and DIDS as follows.

Proposition 4.1. *The FIDS (or DIDS) has $\mathcal{O}(NN_{exp})$ (or $\mathcal{O}(NM)$) memory requirement and $\mathcal{O}(MN(\log N + N_{exp}))$ (or $\mathcal{O}(MN(\log N + M))$) computational complexity.*

5. Numerical experiments

In this section, the numerical experiments are presented to achieve our two-fold objective. They show that the proposed FIDS and DIDS can indeed converge with the theoretical accuracy in both space and time. Meanwhile, they assess the computational efficiency and theoretical results on circulant preconditioners described in Section 4. For the Krylov subspace method and direct solver, we exploit built-in functions for the preconditioned BiCGSTAB (PBiCGSTAB) method [58] (in Example 2) and MATLAB's backslash in Examples 1–2, respectively. For the BiCGSTAB method with circulant preconditioners, the stopping criterion of those methods is $\|\mathbf{r}^{(k)}\|_2/\|\mathbf{r}^{(0)}\|_2 < \text{tol} = 10^{-10}$, where $\mathbf{r}^{(k)}$ is the residual vector of the linear system after k iterations, and the initial guess is chosen as the zero vector. All experiments were performed on a Windows 10 (64 bit) PC-Intel(R) Core(TM) i5-8265U CPU (1.6 ~ 3.9 GHz), 8 GB of RAM using MATLAB 2017b with machine epsilon 10^{-16} in double precision floating point arithmetic. By the way, all timings are averages over 20 runs of our algorithms. We also choose the tolerance error $\epsilon = 10^{-10}$, 10^{-9} for FIDS in Examples 1–2, respectively. Moreover, some notations on numerical errors are introduced as follows:

$$\text{Error}_\infty(N, M) = \max_{0 \leq j \leq M} \|\mathbf{E}^j\|_\infty \quad \text{and} \quad \text{Error}_2(N, M) = \max_{0 \leq j \leq M} \|\mathbf{E}^j\|_2,$$

then

$$\text{Rate}_\infty = \begin{cases} \log_2 \left(\frac{\text{Error}_\infty(N(M/2), M/2)}{\text{Error}_\infty(N(M), M)} \right), & \text{(temporal convergence order),} \\ \log_2 \left(\frac{\text{Error}_\infty(N/2, M(N/2))}{\text{Error}_\infty(N, M(N))} \right), & \text{(spatial convergence order),} \end{cases}$$

and

$$\text{Rate}_2 = \begin{cases} \log_2 \left(\frac{\text{Error}_2(N(M/2), M/2)}{\text{Error}_2(N(M), M)} \right), & \text{(temporal convergence order),} \\ \log_2 \left(\frac{\text{Error}_2(N/2, M(N/2))}{\text{Error}_2(N, M(N))} \right), & \text{(spatial convergence order).} \end{cases}$$

Example 1. (Accuracy test) In this example, we consider the Eq. (1.1) with the spatial domain $\Omega = (-1, 1)$ and the time interval $[0, T] = [0, 1]$. The diffusion coefficients $\kappa(x, t) =$

$(1+t)e^{0.8x+1}$ and the source term is given

$$f(x, t) = \Gamma(1 + \gamma)(1 - x^2)^{s+\alpha/2} + \kappa(x, t) \frac{2^\alpha \Gamma(\frac{\alpha+1}{2}) \Gamma(s + 1 + \alpha/2)}{\sqrt{\pi} \Gamma(s + 1)} \times \\ {}_2F_1\left(\frac{\alpha + 1}{2}, -s; \frac{1}{2}; x^2\right) (t^\gamma + 1), \quad s \in \mathbb{N}^+,$$

where ${}_2F_1(\cdot)$ denotes the Gauss hypergeometric function which can be computed via the MATLAB built-in function ‘hypergeom.m’ and the initial-boundary value conditions are

$$u(-1, t) = u(1, t) = 0, \quad \text{and} \quad u(x, 0) = (1 - x^2)^{s+\alpha/2}.$$

Thus the exact solution of this problem is $u(x, t) = (1 - x^2)^{s+\alpha/2}(t^\gamma + 1)$. The numerical results involving both spatial and temporal convergence orders of FIDS (3.3) and DIDS (3.4) are shown in Tables 1–6 and Figures 1–2. Here it should be mentioned that we only use the direct method for solving the resultant linear systems of FIDS (3.3) and DIDS (3.4), respectively, because the maximal size of such resultant linear systems is still *smaller* than 128 and the superiority of Krylov subspace solvers with circulant preconditioners are slightly less remarkable compared to the direct solvers in terms of the elapsed CPU time; see e.g., to [29, 55] and the context in the next example for a discussion.

Table 1: The L_∞ - and L_2 -norm of errors, temporal convergence orders for solving Example 1 with $\alpha = 1.5$, $N(M) = \lceil 2M^{\min\{r\gamma, 2-\gamma\}/2} \rceil$, $\mu = 1 + \frac{\alpha}{2}$, $\kappa_\mu = 1$, and $s = 3$.

(r, γ)	M	DIDS (3.4)					FIDS (3.3)				
		Err $_\infty$	Rate	Err $_2$	Rate	CPU(s)	Err $_\infty$	Rate	Err $_2$	Rate	CPU(s)
(1,0.8)	2^8	6.734e-3	–	5.974e-3	–	0.068	6.734e-3	–	5.974e-3	–	0.051
	2^9	3.639e-3	0.888	3.173e-3	0.913	0.182	3.639e-3	0.888	3.173e-3	0.913	0.103
	2^{10}	1.972e-3	0.884	1.698e-3	0.902	0.619	1.972e-3	0.884	1.698e-3	0.902	0.204
	2^{11}	1.108e-3	0.832	9.450e-4	0.845	2.712	1.108e-3	0.832	9.450e-4	0.845	0.702
(2,0.5)	2^7	4.363e-3	–	3.827e-3	–	0.026	4.363e-3	–	3.827e-3	–	0.028
	2^8	1.964e-3	1.152	1.692e-3	1.177	0.047	1.964e-3	1.152	1.692e-3	1.177	0.059
	2^9	9.497e-4	1.048	8.124e-4	1.059	0.163	9.497e-4	1.048	8.124e-4	1.059	0.152
	2^{10}	4.542e-4	1.064	3.934e-4	1.046	0.732	4.542e-4	1.064	3.934e-4	1.046	0.473
(3,0.8)	2^7	1.473e-3	–	1.304e-3	–	0.028	1.473e-3	–	1.304e-3	–	0.045
	2^8	5.980e-4	1.301	5.251e-4	1.312	0.074	5.980e-4	1.301	5.251e-4	1.312	0.096
	2^9	2.459e-4	1.282	2.136e-4	1.297	0.287	2.459e-4	1.282	2.136e-4	1.297	0.276
	2^{10}	1.037e-4	1.246	8.954e-5	1.255	1.056	1.037e-4	1.246	8.954e-5	1.255	0.834

Tables 1–4 present the numerical errors, CPU time (in seconds) and spatial/temporal convergence rates of both FIDS and DIDS for solving the problem (1.1), which satisfy the smooth condition mentioned in Remark 3.1. With the changes of discretized grid size, it is easily seen that for the temporal direction, the numerical convergence order is consistent with the theoretical estimate $\mathcal{O}(N^{-\min\{r\gamma, 2-\gamma\}})$ for different α 's. Meanwhile, it can find that the numerically spatial convergence order is exactly consistent with the theoretical estimation $\mathcal{O}(h^2)$ for different orders of the IFL. In addition, the results of average CPU time

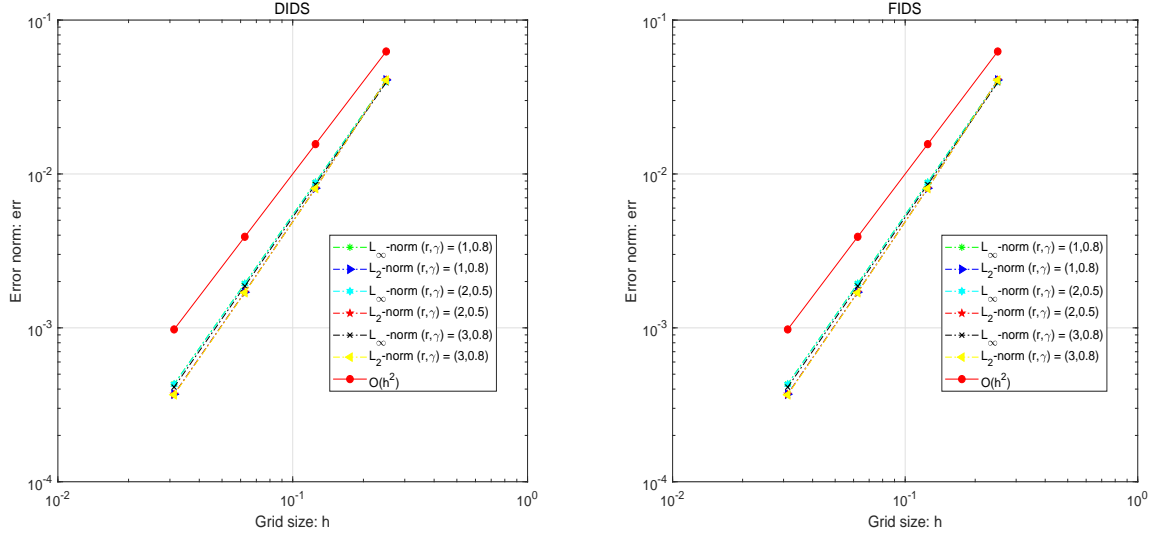


Fig. 1: The spatial convergence order of two difference schemes for Example 1 with $\alpha = 1.6$, $M(N) = \lceil (N/2)^{2/\min\{r\gamma, 2-\gamma\}} \rceil$, $\mu = 2$, $\kappa_\mu = 2$, and $s = 3$. Left: DIDS (3.4); Right: FIDS (3.3).

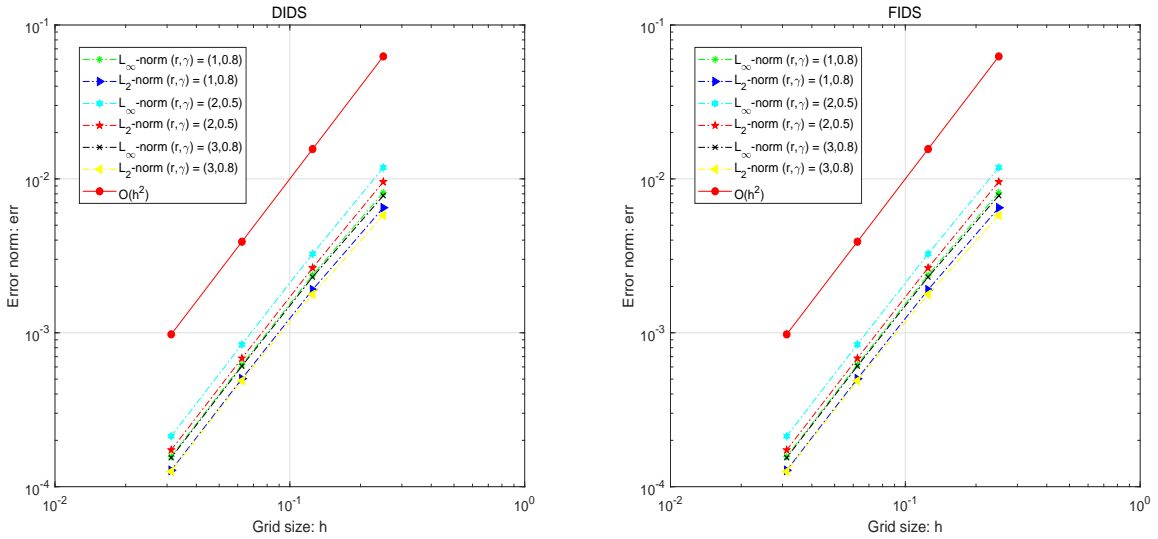


Fig. 2: The spatial convergence order of two difference schemes for Example 1 with $\alpha = 0.4$, $M(N) = \lceil (N/2)^{2/\min\{r\gamma, 2-\gamma\}} \rceil$, $\mu = 2$, $\kappa_\mu = 2$, and $s = 3$. Left: DIDS (3.4); Right: FIDS (3.3).

Table 2: The L_∞ - and L_2 -norm of errors, temporal convergence orders for solving Example 1 with $\alpha = 0.5$, $N(M) = \lceil 2M^{\min\{r\gamma, 2-\gamma\}/2} \rceil$, $\mu = 1 + \frac{\alpha}{2}$, $\kappa_\mu = 1$, and $s = 3$.

(r, γ)	M	DIDS (3.4)					FIDS (3.3)				
		Err_∞	Rate	Err_2	Rate	CPU(s)	Err_∞	Rate	Err_2	Rate	CPU(s)
(1,0.8)	2^8	2.222e-3	–	1.908e-3	–	0.058	2.222e-3	–	1.908e-3	–	0.045
	2^9	1.240e-3	0.842	1.060e-3	0.847	0.176	1.240e-3	0.842	1.060e-3	0.847	0.096
	2^{10}	6.942e-4	0.837	5.918e-4	0.841	0.589	6.942e-4	0.837	5.918e-4	0.841	0.196
	2^{11}	4.022e-4	0.787	3.420e-4	0.791	2.654	4.022e-4	0.787	3.420e-4	0.791	0.558
(2,0.5)	2^7	1.608e-3	–	1.318e-3	–	0.023	1.608e-3	–	1.318e-3	–	0.032
	2^8	8.214e-4	0.969	6.694e-4	0.977	0.046	8.214e-4	0.969	6.694e-4	0.977	0.061
	2^9	4.171e-4	0.978	3.405e-4	0.975	0.181	4.171e-4	0.978	3.405e-4	0.975	0.147
	2^{10}	2.112e-4	0.982	1.718e-4	0.987	0.747	2.112e-4	0.982	1.718e-4	0.987	0.454
(3,0.8)	2^7	4.389e-4	–	4.389e-4	–	0.029	4.389e-4	–	4.389e-4	–	0.041
	2^8	1.869e-4	1.232	1.845e-4	1.250	0.072	1.869e-4	1.232	1.845e-4	1.250	0.101
	2^9	8.001e-5	1.224	7.874e-5	1.228	0.281	8.001e-5	1.224	7.874e-5	1.228	0.273
	2^{10}	3.492e-5	1.196	3.439e-5	1.195	1.073	3.492e-5	1.196	3.439e-5	1.195	0.826

Table 3: The L_∞ - and L_2 -norm of errors, spatial convergence orders for solving Example 1 with $\alpha = 1.5$, $M(N) = \lceil (N/2)^{2/\min\{r\gamma, 2-\gamma\}} \rceil$, $\mu = 1 + \frac{\alpha}{2}$, $\kappa_\mu = 1$, and $s = 3$.

(r, γ)	N	DIDS (3.4)					FIDS (3.3)				
		Err_∞	Rate	Err_2	Rate	CPU(s)	Err_∞	Rate	Err_2	Rate	CPU(s)
(1,0.8)	2^3	3.889e-2	–	3.802e-2	–	0.009	3.889e-2	–	3.802e-2	–	0.008
	2^4	8.668e-3	2.166	7.760e-3	2.293	0.031	8.668e-3	2.166	7.760e-3	2.293	0.030
	2^5	1.972e-3	2.136	1.698e-3	2.193	0.587	1.972e-3	2.136	1.698e-3	2.193	0.256
	2^6	4.561e-4	2.112	3.846e-4	2.142	20.161	4.561e-4	2.112	3.846e-4	2.142	1.727
(2,0.5)	2^3	3.865e-2	–	3.789e-2	–	0.003	3.865e-2	–	3.789e-2	–	0.005
	2^4	8.625e-3	2.164	7.734e-3	2.293	0.010	8.625e-3	2.164	7.734e-3	2.293	0.016
	2^5	1.964e-3	2.135	1.692e-3	2.192	0.045	1.964e-3	2.135	1.692e-3	2.192	0.068
	2^6	4.542e-4	2.112	3.834e-4	2.142	0.736	4.542e-4	2.112	3.834e-4	2.142	0.457
(3,0.8)	2^3	3.766e-2	–	3.791e-2	–	0.002	3.766e-2	–	3.791e-2	–	0.004
	2^4	8.349e-3	2.174	7.710e-3	2.298	0.006	8.349e-3	2.174	7.710e-3	2.298	0.009
	2^5	1.889e-3	2.144	1.682e-3	2.197	0.015	1.889e-3	2.144	1.682e-3	2.197	0.032
	2^6	4.351e-4	2.119	3.801e-4	2.145	0.108	4.351e-4	2.119	3.801e-4	2.145	0.152

demonstrate that the FIDS has the overwhelming performance over the DIDS, especially for the large integer M .

On the other hand, there is another splitting parameter $\mu = 2$ for discretizing the IFL, and it makes the spatial discretization of IFL enjoy the second-order accuracy [37]. According to Tables 5–6 and Figures 1–2, it is not hard to find that both FIDS and DIDS under such a spatial discretization for solving Example 1 can reach still the spatial convergence order $\mathcal{O}(h^2)$ and $\mathcal{O}(N^{-\min\{r\gamma, 2-\gamma\}})$ with different settings. Thus such results are also consistent with the theoretical estimate described in Section 3.2. Again, the results of average elapsed CPU time show that the FIDS has the overwhelming performance over the DIDS, especially for the large integer M .

Example 2. The second example is similar to the setting in Example 1, while we choose

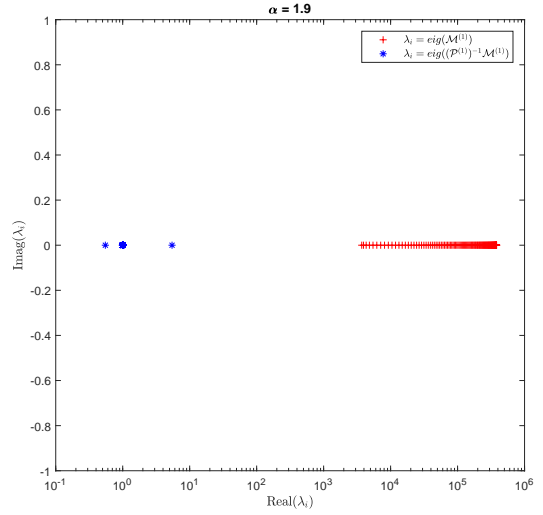
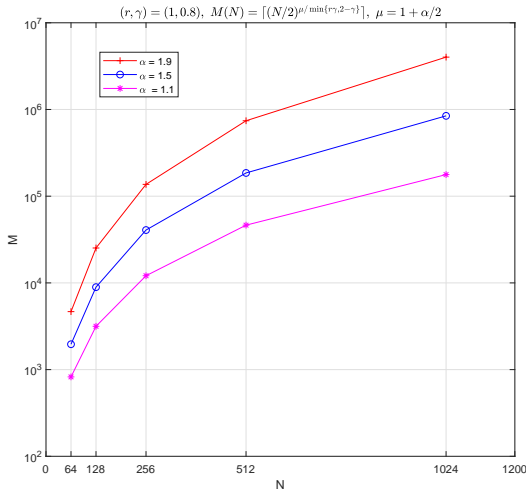
Table 4: The L_∞ - and L_2 -norm of errors, spatial convergence orders for solving Example 1 with $\alpha = 0.5$, $M(N) = \lceil (N/2)^{2/\min\{r\gamma, 2-\gamma\}} \rceil$, $\mu = 1 + \frac{\alpha}{2}$, $\kappa_\mu = 1$, and $s = 3$.

(r, γ)	N	DIDS (3.4)					FIDS (3.3)				
		Err_∞	Rate	Err_2	Rate	CPU(s)	Err_∞	Rate	Err_2	Rate	CPU(s)
(1,0.8)	2^3	1.197e-2	–	1.039e-2	–	0.007	1.197e-2	–	1.039e-2	–	0.005
	2^4	2.822e-3	2.085	2.429e-3	2.097	0.030	2.822e-3	2.085	2.429e-3	2.097	0.029
	2^5	6.942e-4	2.023	5.918e-4	2.037	0.583	6.942e-4	2.023	5.918e-4	2.037	0.247
	2^6	1.730e-4	2.005	1.467e-4	2.013	20.156	1.730e-4	2.005	1.467e-4	2.013	1.731
(2,0.5)	2^3	1.167e-2	–	1.021e-2	–	0.003	1.167e-2	–	1.021e-2	–	0.004
	2^4	3.092e-3	1.917	2.559e-3	1.996	0.012	3.092e-3	1.917	2.559e-3	1.996	0.014
	2^5	8.214e-4	1.912	6.694e-4	1.935	0.044	8.214e-4	1.912	6.694e-4	1.935	0.062
	2^6	2.112e-4	1.960	1.718e-4	1.963	0.734	2.112e-4	1.960	1.718e-4	1.963	0.448
(3,0.8)	2^3	9.872e-3	–	9.697e-3	–	0.002	9.872e-3	–	9.697e-3	–	0.004
	2^4	2.303e-3	2.100	2.264e-3	2.099	0.005	2.303e-3	2.100	2.264e-3	2.099	0.007
	2^5	5.584e-4	2.044	5.493e-4	2.043	0.016	5.584e-4	2.044	5.493e-4	2.043	0.029
	2^6	1.379e-4	2.017	1.359e-4	2.016	0.104	1.379e-4	2.017	1.359e-4	2.016	0.139

$s = 1$ and $\kappa(x, t) = 7[\ln(5 + 2x + t) + \cos(xt)]/4$. Then the exact solution $u(x, t)$ and source term $f(x, t)$ can be computed via the form described in Example 1, and the corresponding initial-boundary conditions are also similarly obtained.

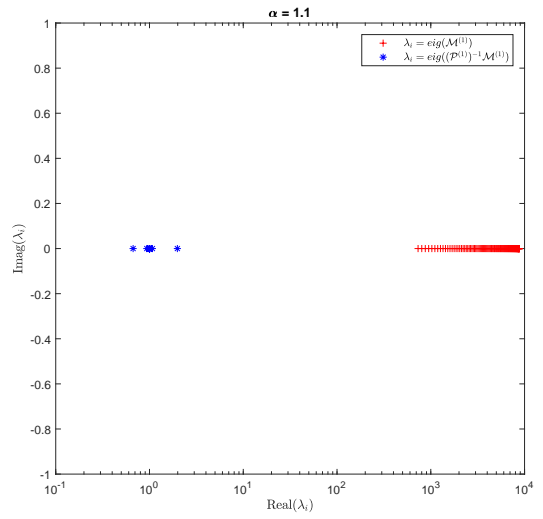
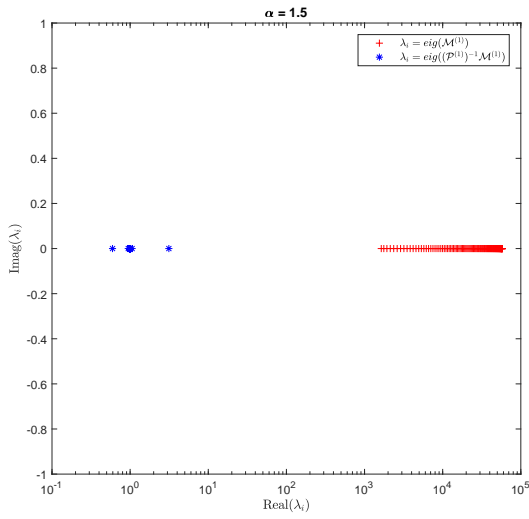
In this example, it note that the exact solution $u(x, \cdot) \in \mathcal{C}^{1, \frac{\alpha}{2}}(\mathbb{R})$ satisfies the less smoother condition than that in Example 1. Moreover, it is seen from Tables 7–10 that for the temporal direction, the numerical convergence rate of both FIDS and DIDS is consistent with the theoretical estimate $\mathcal{O}(N^{-\min\{r\gamma, 2-\gamma\}})$ for different settings. However, it remarked that the spatial convergence rate of both FIDS and DIDS can at least approach to $1 + \frac{\alpha}{2}$, especially when α increasingly goes to 2, the spatial convergence orders of both FIDS and DIDS are almost 2. These results on spatial convergence rate of both FIDS and DIDS are fairly better than the theoretical estimate in Remark 3.1. It implies that the error analysis and smooth condition of the numerical discretization of IFL used to establish the IDS can be further sharpened and weakened, respectively. Analogously, the average CPU time of FIDS will be smaller than that of DIDS for solving the problem (1.1), when the number of time levels is increasingly large.

On the other hand, Table 11 and Figs. 3–4 are carried out to show the effectiveness of the proposed circulant preconditioners, especially which is useful for the order α ($\rightarrow 2$) of IFL; refer to Figs. 3–4 as well. For Fig. 3-(a), it implies that if we increase N , then the number of time level will be too huge to make a concise comparison of FIDS and DIDS (with no/circulant preconditioners). Moreover, due to the large number M , the family of FIDS should be more efficient than the counterparts of DIDS for solving the problem (1.1). As seen from Table 11, it finds that the proposed circulant preconditioner is efficient to accelerate the implementations of both FIDS and DIDS in terms of the reduction of “Its” and “CPU”, especially for large integers M and N . This observation can be also supported by the clustering eigenvalue distributions shown in Figs. 3–4. Moreover, the number of iterations of “DIDS + \mathcal{P} ” and “FIDS + \mathcal{P} ” is roughly independent of decreasing spatial grid size. The above results of circulant preconditioners are exactly consistent with the



(a) The number of time levels M versus the number of spatial grid nodes (N) for $(r, \gamma) = (1, 0.8)$.

(b) The eigenvalue distributions of original and pre-conditioned matrices when $\alpha = 1.9$.



(c) The eigenvalue distributions of original and pre-conditioned matrices when $\alpha = 1.5$.

(d) The eigenvalue distributions of original and pre-conditioned matrices when $\alpha = 1.1$.

Fig. 3: The brief performance analysis of FIDS (3.3) and DIDS (3.4) with no/circulant preconditioners for solving Example 2 with $N = 2^7$ in the subfigures: (b)–(d).

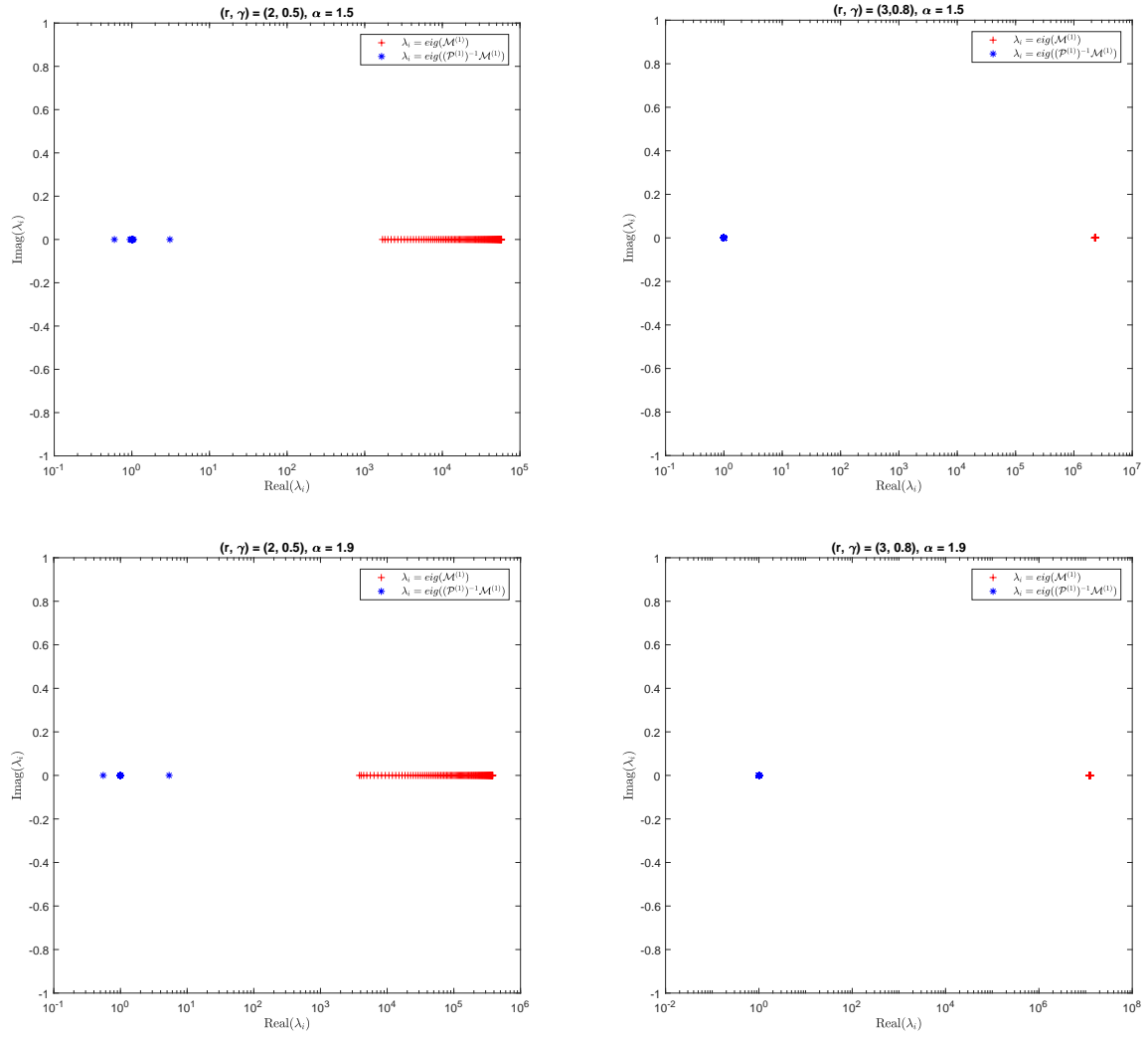


Fig. 4: Eigenvalue distributions of the original and preconditioned matrices from both FIDS (3.3) and DIDS (3.4) for Example 2 with different setting and $N = 2^7$.

Table 5: The L_∞ - and L_2 -norm of errors, temporal convergence orders for solving Example 1 with $\alpha = 1.6$, $N(M) = \lceil 2M^{\min\{r\gamma, 2-\gamma\}/2} \rceil$, $\mu = 2$, $\kappa_\mu = 2$, and $s = 3$

(r, γ)	M	DIDS (3.4)					FIDS (3.3)				
		Err_∞	Rate	Err_2	Rate	CPU(s)	Err_∞	Rate	Err_2	Rate	CPU(s)
(1,0.8)	2^8	6.826e-3	–	6.184e-3	–	0.067	6.826e-3	–	6.184e-3	–	0.048
	2^9	3.640e-3	0.907	3.238e-3	0.934	0.183	3.640e-3	0.907	3.238e-3	0.934	0.103
	2^{10}	1.943e-3	0.906	1.705e-3	0.925	0.614	1.943e-3	0.906	1.705e-3	0.925	0.199
	2^{11}	1.075e-3	0.854	9.345e-4	0.868	2.710	1.075e-3	0.854	9.345e-4	0.868	0.687
(2,0.5)	2^7	4.385e-3	–	3.924e-3	–	0.022	4.385e-3	–	3.924e-3	–	0.028
	2^8	1.935e-3	1.180	1.701e-3	1.206	0.044	1.935e-3	1.180	1.701e-3	1.206	0.064
	2^9	9.178e-4	1.076	8.005e-4	1.087	0.176	9.178e-4	1.076	8.005e-4	1.087	0.155
	2^{10}	4.298e-4	1.095	3.697e-4	1.115	0.734	4.298e-4	1.095	3.697e-4	1.115	0.438
(3,0.8)	2^7	1.445e-3	–	1.304e-3	–	0.028	1.445e-3	–	1.304e-3	–	0.047
	2^8	5.716e-4	1.338	5.120e-4	1.349	0.076	5.716e-4	1.338	5.120e-4	1.349	0.099
	2^9	2.288e-4	1.321	2.029e-4	1.336	0.279	2.288e-4	1.321	2.029e-4	1.336	0.271
	2^{10}	9.389e-5	1.285	8.279e-5	1.293	1.059	9.389e-5	1.285	8.279e-5	1.293	0.832

Table 6: The L_∞ - and L_2 -norm of errors, temporal convergence orders for solving Example 1 with $\alpha = 0.4$, $N(M) = \lceil 2M^{\min\{r\gamma, 2-\gamma\}/2} \rceil$, $\mu = 2$, $\kappa_\mu = 2$, and $s = 3$

(r, γ)	M	DIDS (3.4)					FIDS (3.3)				
		Err_∞	Rate	Err_2	Rate	CPU(s)	Err_∞	Rate	Err_2	Rate	CPU(s)
(1,0.8)	2^8	1.829e-3	–	1.468e-3	–	0.061	1.829e-3	–	1.468e-3	–	0.046
	2^9	1.070e-3	0.774	8.633e-4	0.766	0.179	1.070e-3	0.774	8.633e-4	0.766	0.094
	2^{10}	6.206e-4	0.785	5.027e-4	0.780	0.592	6.206e-4	0.785	5.027e-4	0.780	0.199
	2^{11}	3.589e-4	0.790	2.911e-4	0.788	2.667	3.589e-4	0.790	2.911e-4	0.788	0.553
(2,0.5)	2^7	1.657e-3	–	1.343e-3	–	0.022	1.657e-3	–	1.343e-3	–	0.033
	2^8	8.409e-4	0.978	6.829e-4	0.976	0.045	8.409e-4	0.978	6.829e-4	0.976	0.062
	2^9	4.233e-4	0.990	3.446e-4	0.987	0.183	4.233e-4	0.990	3.446e-4	0.987	0.151
	2^{10}	2.128e-4	0.992	1.731e-4	0.993	0.744	2.128e-4	0.992	1.731e-4	0.993	0.448
(3,0.8)	2^7	4.758e-4	–	3.854e-4	–	0.029	4.758e-4	–	3.854e-4	–	0.042
	2^8	2.071e-4	1.200	1.687e-4	1.193	0.070	2.071e-4	1.200	1.687e-4	1.193	0.101
	2^9	8.963e-5	1.208	7.315e-5	1.205	0.279	8.963e-5	1.208	7.315e-5	1.205	0.268
	2^{10}	3.930e-5	1.190	3.212e-5	1.187	1.069	3.930e-5	1.190	3.212e-5	1.187	0.821

theoretical investigations given in Section 4. In one word, the “FIDS + \mathcal{P} ” is the most promising numerical method for solving the problem (1.1), especially with large integers M , N and $M > N$.

6. Conclusions

In this work, we proposed two fast and easy-to-implement IDSs (i.e., FIDS and DIDS) for solving the TSFDE (1.1) with non-smooth initial data, which was not well-studied in the previous work. Meanwhile, both the solvability, stability and convergence rate of the proposed IDSs utilized non-uniform temporal steps are strictly proved via the matrix properties, which are meticulously derived from the direct discretization of IFL. Numerical results in Section 5 are reported to support our theoretical findings. In addition, although the focus is

Table 7: The L_∞ - and L_2 -norm of errors, temporal convergence orders for solving Example 2 with $\alpha = 1.9$, $N(M) = \lceil 2M^{\min\{r\gamma, 2-\gamma\}/\mu} \rceil$, $\mu = 1 + \frac{\alpha}{2}$ and $\kappa_\mu = 1$.

(r, γ)	M	DIDS (3.4)					FIDS (3.3)				
		Err_∞	Rate	Err_2	Rate	CPU(s)	Err_∞	Rate	Err_2	Rate	CPU(s)
(1,0.8)	2^8	1.724e-2	–	1.839e-2	–	0.054	1.724e-2	–	1.839e-2	–	0.046
	2^9	9.887e-3	0.803	1.056e-2	0.801	0.178	9.887e-3	0.803	1.056e-2	0.801	0.102
	2^{10}	5.300e-3	0.900	5.664e-3	0.898	0.703	5.300e-3	0.900	5.664e-3	0.898	0.256
	2^{11}	2.997e-3	0.823	3.210e-3	0.819	2.586	2.997e-3	0.823	3.210e-3	0.819	0.487
(2,0.5)	2^7	1.061e-2	–	1.132e-2	–	0.014	1.061e-2	–	1.132e-2	–	0.026
	2^8	5.231e-3	1.021	5.595e-3	1.017	0.054	5.231e-3	1.021	5.595e-3	1.017	0.059
	2^9	2.488e-3	1.072	2.668e-3	1.068	0.152	2.488e-3	1.072	2.668e-3	1.068	0.141
	2^{10}	1.241e-3	1.004	1.334e-3	1.001	0.721	1.241e-3	1.004	1.334e-3	1.001	0.457
(3,0.8)	2^7	3.951e-3	–	4.234e-3	–	0.019	3.951e-3	–	4.234e-3	–	0.046
	2^8	1.645e-3	1.264	1.767e-3	1.260	0.066	1.645e-3	1.264	1.767e-3	1.260	0.098
	2^9	6.895e-4	1.255	7.427e-4	1.251	0.272	6.895e-4	1.255	7.427e-4	1.251	0.267
	2^{10}	2.851e-4	1.274	3.079e-4	1.270	1.100	2.851e-4	1.274	3.079e-4	1.270	0.824

on the case of the one-dimensional spatial domain in this work, we note that the proposed methods utilizing spatial discretizations [38] can be directly adopted and corresponding results remain valid for two- and three-dimensional cases, which will be precisely presented in our another coming manuscript.

On the other hand, due to the nonlocality of Caputo fractional derivative in the TSFDE (1.1), the numerical scheme needs to repeat the weighted sum of solutions in previous time levels. In order to reduce the computational cost, we exploit the fast SOE approximation of graded $L1$ formula to result in the FIDS, which will be cheaper than the DIDS, especially for large integer M . However, no matter FIDS or DIDS, they both need to solve the dense discretized systems, which are still time-consuming. It implies that the efficient implementation of FIDS and DIDS should be further considered. With the help of Toeplitz-like matrix, we construct the BiCGSTAB with circulant preconditioners for solving the series of discretized linear systems (cf. Eq. 3.5 and Eq. 4.1)) without storing any matrices. It makes the FIDS (or DIDS) only require $\mathcal{O}(NN_{exp})$ (or $\mathcal{O}(NM)$) memory requirement and $\mathcal{O}(MN(\log N + N_{exp}))$ (or $\mathcal{O}(MN(\log N + M))$) computational complexity. To ensure the circulant preconditioners efficient, we theoretically show that the eigenvalues of preconditioned matrices cluster around 1, expect for few outliers. The vast majority of these eigenvalues are well separated away from 0. It means that the BiCGSTAB with circulant preconditioners for solving the discretized linear systems can converge very fast. Numerical experiments are reported to show the effectiveness of the FIDS and DIDS with PBiCGSTAB solvers in terms of the elapsed CPU time and number of iterations, especially the former one.

Finally, it is meaningful to note that the numerically spatial convergence order of FIDS or DIDS is better than the theoretical estimate of FIDS or DIDS, cf. Example 2. It means that the error analysis of numerical schemes for solving time-dependent problems is different from the numerical IFL introduced in [37]. The more refined error/convergence analysis of FIDS or DIDS is worth exploring in our future work; refer e.g., to [38, 40, 41] for a discussion. Our current work includes applying the FIDS and DIDS for solving the (nonlinear) multi-

Table 8: The L_∞ - and L_2 -norm of errors, temporal convergence orders for solving Example 2 with $\alpha = 0.5$, $N(M) = \lceil 2M^{\min\{r\gamma, 2-\gamma\}/\mu} \rceil$, $\mu = 1 + \frac{\alpha}{2}$ and $\kappa_\mu = 1$.

(r, γ)	M	DIDS (3.4)					FIDS (3.3)				
		Err_∞	Rate	Err_2	Rate	CPU(s)	Err_∞	Rate	Err_2	Rate	CPU(s)
(1,0.8)	2^8	1.699e-3	–	1.698e-3	–	0.077	1.699e-3	–	1.698e-3	–	0.084
	2^9	1.016e-3	0.742	1.011e-3	0.747	0.321	1.016e-3	0.742	1.011e-3	0.747	0.217
	2^{10}	6.013e-4	0.757	5.980e-4	0.758	1.235	6.013e-4	0.757	5.980e-4	0.758	0.660
	2^{11}	3.521e-4	0.772	3.496e-4	0.774	5.899	3.521e-4	0.772	3.496e-4	0.774	2.759
(2,0.5)	2^7	1.619e-3	–	1.609e-3	–	0.031	1.619e-3	–	1.609e-3	–	0.050
	2^8	8.238e-4	0.975	8.174e-4	0.977	0.158	8.238e-4	0.975	8.174e-4	0.977	0.173
	2^9	4.189e-4	0.976	4.157e-4	0.975	0.979	4.189e-4	0.976	4.157e-4	0.975	0.887
	2^{10}	2.115e-4	0.986	2.098e-4	0.987	10.409	2.115e-4	0.986	2.098e-4	0.987	9.215
(3,0.8)	2^5	1.274e-3	–	1.340e-3	–	0.011	1.274e-3	–	1.340e-3	–	0.012
	2^6	5.719e-4	1.156	5.970e-4	1.166	0.025	5.719e-4	1.156	5.970e-4	1.166	0.038
	2^7	2.529e-4	1.178	2.627e-4	1.185	0.102	2.529e-4	1.178	2.627e-4	1.185	0.130
	2^8	1.109e-4	1.189	1.149e-4	1.193	1.426	1.109e-4	1.189	1.149e-4	1.193	1.347

dimensional TSFDEs (on unbounded domains) with nonhomogeneous boundary conditions, and designing the more efficient preconditioning techniques, such as τ -algebra, multigrid [55] and banded preconditioners, for the corresponding two- and three-level Toeplitz discretized linear systems.

Acknowledgement

This research is supported by NSFC (11801463), the Fundamental Research Funds for the Central Universities (JBK1902028 and JBK1805001), and the Ministry of Education of Humanities and Social Science Layout Project (19JYA790094).

References

- [1] I. Podlubny, *Fractional Differential Equations*, Academic Press, New York, NY (1999).
- [2] H.G. Sun, Y. Zhang, D. Baleanu, W. Chen, Y.Q. Chen, A new collection of real world applications of fractional calculus in science and engineering, *Commun. Nonlinear Sci. Numer. Simul.*, 64 (2018), pp. 213-231.
- [3] J.L. Vázquez, The Mathematical Theories of Diffusion: Nonlinear and Fractional Diffusion, in: *Nonlocal and Nonlinear Diffusions and Interactions: New Methods and Directions* (M. Bonforte, G. Grillo, eds.), Lecture Notes in Mathematics, vol. 2186, Springer, Cham, Switzerland (2017), pp. 205-278. DOI: 10.1007/978-3-319-61494-6_5.
- [4] C. Li, Q. Yi, Modeling and computing of fractional convection equation, *Commun. Appl. Math. Comput.*, 1(4) (2019), pp. 565-595.
- [5] W. Chen, H. Sun, X. Zhang, D. Korošak, Anomalous diffusion modeling by fractal and fractional derivatives, *Comput. Math. Appl.*, 59(5) (2010), pp. 1754-1758.
- [6] M.F. Shlesinger, B.J. West, J. Klafter, Lévy dynamics of enhanced diffusion: application to turbulence, *Phys. Rev. Lett.*, 58(11) (1987), pp. 1100-1103.
- [7] G. Estrada-Rodriguez, H. Gimperlein, K.J. Painter, J. Stoczek, Space-time fractional diffusion in cell movement models with delay, *Math. Models Meth. Appl. Sci.*, 29(1) (2019), pp. 65-88.

Table 9: The L_∞ - and L_2 -norm of errors, spatial convergence orders for solving Example 2 with $\alpha = 1.9$, $M(N) = \lceil (N/2)^{\mu/\min\{r\gamma, 2-\gamma\}} \rceil$, $\mu = 1 + \frac{\alpha}{2}$ and $\kappa_\mu = 1$.

(r, γ)	N	DIDS (3.4)					FIDS (3.3)				
		Err_∞	Rate	Err_2	Rate	CPU(s)	Err_∞	Rate	Err_2	Rate	CPU(s)
(1,0.8)	9	7.770e-2	–	8.304e-2	–	0.006	7.770e-2	–	8.304e-2	–	0.007
	18	1.929e-2	2.010	2.052e-2	2.017	0.035	1.929e-2	2.010	2.052e-2	2.017	0.033
	36	4.719e-3	2.031	5.045e-3	2.024	0.834	4.719e-3	2.031	5.045e-3	2.024	0.254
	72	1.153e-3	2.033	1.238e-3	2.026	23.551	1.153e-3	2.033	1.238e-3	2.026	1.927
(2,0.5)	9	7.663e-2	–	8.193e-2	–	0.002	7.663e-2	–	8.193e-2	–	0.005
	18	1.903e-2	2.010	2.026e-2	2.016	0.008	1.903e-2	2.010	2.026e-2	2.016	0.014
	36	4.657e-3	2.031	4.983e-3	2.023	0.053	4.657e-3	2.031	4.983e-3	2.023	0.077
	72	1.138e-3	2.033	1.223e-3	2.026	0.879	1.138e-3	2.033	1.223e-3	2.026	0.426
(3,0.8)	9	7.663e-2	–	8.195e-2	–	0.002	7.663e-2	–	8.195e-2	–	0.004
	18	1.902e-2	2.011	2.025e-2	2.017	0.005	1.902e-2	2.011	2.025e-2	2.017	0.008
	36	4.650e-3	2.032	4.977e-3	2.025	0.016	4.650e-3	2.032	4.977e-3	2.025	0.033
	72	1.135e-3	2.034	1.221e-3	2.028	0.114	1.135e-3	2.034	1.221e-3	2.028	0.162

Table 10: The L_∞ - and L_2 -norm of errors, spatial convergence orders for solving Example 2 with $\alpha = 0.5$, $M(N) = \lceil (N/2)^{\mu/\min\{r\gamma, 2-\gamma\}} \rceil$, $\mu = 1 + \frac{\alpha}{2}$ and $\kappa_\mu = 1$

(r, γ)	N	DIDS (3.4)					FIDS (3.3)				
		Err_∞	Rate	Err_2	Rate	CPU(s)	Err_∞	Rate	Err_2	Rate	CPU(s)
(1,0.8)	2^6	1.871e-3	–	1.871e-3	–	0.065	1.871e-3	–	1.871e-3	–	0.063
	2^7	8.355e-4	1.163	8.323e-4	1.169	0.539	8.355e-4	1.163	8.323e-4	1.169	0.364
	2^8	3.642e-4	1.198	3.616e-4	1.203	5.365	3.642e-4	1.198	3.616e-4	1.203	2.438
	2^9	1.556e-4	1.227	1.543e-4	1.229	88.190	1.556e-4	1.227	1.543e-4	1.229	51.194
(2,0.5)	2^6	2.666e-3	–	2.654e-3	–	0.013	2.666e-3	–	2.654e-3	–	0.023
	2^7	1.157e-3	1.204	1.149e-3	1.208	0.073	1.157e-3	1.204	1.149e-3	1.208	0.091
	2^8	4.970e-4	1.219	4.933e-4	1.219	0.584	4.970e-4	1.219	4.933e-4	1.219	0.571
	2^9	2.115e-4	1.232	2.098e-4	1.234	9.855	2.115e-4	1.232	2.098e-4	1.234	9.277
(3,0.8)	2^5	2.581e-3	–	2.739e-3	–	0.003	2.581e-3	–	2.739e-3	–	0.006
	2^6	1.114e-3	1.211	1.169e-3	1.228	0.007	1.114e-3	1.211	1.169e-3	1.228	0.014
	2^7	4.677e-4	1.253	4.874e-4	1.262	0.025	4.677e-4	1.253	4.874e-4	1.262	0.046
	2^8	2.000e-4	1.226	2.075e-4	1.232	0.161	2.000e-4	1.226	2.075e-4	1.232	0.232

- [8] G. Chi, G. Li, C. Sun, X. Jia, Numerical solution to the space-time fractional diffusion equation and inversion for the space-dependent diffusion coefficient, *J. Comput. Theor. Trans.*, 46(2) (2017), pp. 122-146.
- [9] Q. Du, M. Gunzburger, R.B. Lehoucq, K. Zhou, Analysis and approximation of nonlocal diffusion problems with volume constraints, *SIAM Rev.*, 54(4) (2012), pp. 667-696.
- [10] Q.-Y. Guan, Z.-M. Ma, Boundary problems for fractional Laplacians, *Stoch. Dynam.*, 5(3) (2005), pp. 385-424.
- [11] X. Tian, Q. Du, M. Gunzburger, Asymptotically compatible schemes for the approximation of fractional Laplacian and related nonlocal diffusion problems on bounded domains, *Adv. Comput. Math.*, 42(6) (2016), pp. 1363-1380.
- [12] S. Duo, H. Wang, Y. Zhang, A comparative study on nonlocal diffusion operators related to the fractional Laplacian, *Discrete Contin. Dyn. Syst.-Ser. B*, 24(1) (2019), pp. 231-256.
- [13] F. del Teso, J. Endal, E.R. Jakobsen, Robust numerical methods for nonlocal (and local) equations of porous medium type. Part II: Schemes and experiments, *SIAM J. Numer. Anal.*, 56(6) (2018), pp.

Table 11: The errors and performance of FIDS and DIDS with direct, iterative and preconditioned iterative solvers for Example 2 with different settings and $M(N) = \lceil (N/2)^{\mu / \min\{r\gamma, 2-\gamma\}} \rceil$, $\mu = 1 + \frac{\alpha}{2}$ and $\kappa_\mu = 1$.

(r, γ, α)	N	Err_∞	Err_2	DIDS	FIDS	DIDS + \mathcal{I}		DIDS + \mathcal{P}		FIDS + \mathcal{I}		FIDS + \mathcal{P}	
				CPU(s)	CPU(s)	Its	CPU(s)	Its	CPU(s)	Its	CPU(s)	Its	CPU(s)
(2,0.5,1.5)	2^6	6.362e-4	7.727e-4	0.162	0.156	44.1	0.658	7.6	0.332	44.1	0.655	7.7	0.347
	2^7	1.542e-4	1.889e-4	1.793	1.014	66.8	5.401	7.9	2.380	66.7	4.693	7.9	1.689
	2^8	4.469e-5	4.643e-5	22.217	7.631	92.7	45.111	8.0	20.777	92.7	30.132	8.0	6.698
	2^9	1.333e-5	1.236e-5	413.96	170.24	125.7	570.75	8.2	285.50	125.7	306.26	8.2	43.338
(3,0.8,1.5)	2^7	1.381e-4	1.734e-4	0.286	0.372	41.5	0.935	6.6	0.446	41.6	0.900	6.6	0.439
	2^8	3.265e-5	4.164e-5	2.931	2.142	48.6	4.479	6.9	2.104	48.6	4.091	6.9	1.545
	2^9	7.897e-6	9.997e-6	44.728	33.845	54.0	35.156	7.0	16.488	53.9	26.938	7.1	8.143
	2^{10}	2.319e-6	2.396e-6	624.02	511.16	57.8	206.13	7.0	138.18	57.8	97.137	7.0	34.543
(2,0.5,1.9)	2^6	1.446e-3	1.553e-3	0.507	0.386	65.6	2.123	7.9	0.853	65.6	1.879	7.9	0.748
	2^7	3.533e-4	3.811e-4	7.831	2.087	116.4	22.072	7.9	8.574	116.4	17.458	7.9	3.838
	2^8	8.636e-5	9.354e-5	194.74	21.665	198.3	275.11	8.1	135.58	198.3	203.71	8.1	18.073
	2^9	2.112e-5	2.297e-5	48229.2	1029.78	316.1	11093.2	8.1	2474.12	316.3	2620.56	8.1	132.04
(3,0.8,1.9)	2^7	3.521e-4	3.800e-4	0.935	0.689	73.8	3.317	7.3	1.201	73.9	3.222	7.3	1.049
	2^8	8.596e-5	9.318e-5	10.468	5.134	100.3	20.579	7.3	7.464	100.2	17.025	7.3	3.679
	2^9	2.100e-5	2.286e-5	173.492	84.047	127.3	246.74	7.4	81.104	127.5	151.45	7.4	21.436
	2^{10}	5.136e-6	5.614e-6	2438.12	1505.84	151.0	1616.83	7.3	1003.78	151.0	714.72	7.3	86.540

- 3611-3647.
- [14] I. Podlubny, A. Chechkin, T. Skovranek, Y.Q. Chen, B.M.V. Jarad, Matrix approach to discrete fractional calculus II: Partial fractional differential equations, *J. Comput. Phys.*, 228(8) (2009), pp. 3137-3153.
 - [15] Q. Yang, F.Liu, I. Turner, Numerical methods for fractional partial differential equations with Riesz space fractional derivatives, *Appl. Math. Model.*, 34 (1) (2010), pp. 200-218.
 - [16] Q. Yang, I. Turner, F. Liu, M. Ilić, Novel numerical methods for solving the time-space fractional diffusion equation in two dimensions, *SIAM J. Sci. Comput.*, 33(3) (2011), pp. 1159-1180.
 - [17] P. Garbaczewski, V. Stephanovich, Fractional Laplacians in bounded domains: Killed, reflected, censored, and taboo Lévy flights, *Phys. Rev. E*, 99(4) (2019), Article No. 042126, 22 pages. DOI: 10.1103/PhysRevE.99.042126.
 - [18] Q.-Y. Guan, Z.-M. Ma, Reflected symmetric α -stable processes and regional fractional Laplacian, *Probab. Theory Rel.*, 134(4) (2006), pp. 649-694.
 - [19] V.N. Kolokoltsov, M.A. Veretennikova, Well-posedness and regularity of the Cauchy problem for nonlinear fractional in time and space equations, *Fractional Differ. Calc.*, 4(1) (2014), pp. 1-30.
 - [20] A. Hanyga, Multi-dimensional solutions of space-time-fractional diffusion equations, *Proc. R. Soc. Lond. A*, 458(2018) (2002), pp. 429-450. DOI: 10.1098/rspa.2001.0893.
 - [21] J.L. Padgett, The quenching of solutions to time-space fractional Kawarada problems, *Comput. Math. Appl.*, 76(7) (2018), pp. 1583-1592.
 - [22] L. Li, J.-G. Liu, L. Wang, Cauchy problems for Keller-Segel type time-space fractional diffusion equation, *J. Differ. Equ.*, 265(3) (2018), pp. 1044-1096.
 - [23] J. Jia, K. Li, Maximum principles for a time-space fractional diffusion equation, *Appl. Math. Lett.*, 62 (2016), pp. 23-28.
 - [24] A. Bonito, W. Lei, J.E. Pasciak, Numerical approximation of space-time fractional parabolic equations, *Comput. Methods Appl. Math.*, 17(4) (2017), pp. 679-705.
 - [25] G. Acosta, F.M. Bersetche, J.P. Borthagaray, Finite element approximations for fractional evolution problems, *Fract. Calc. Appl. Anal.*, 22(3) (2019), pp. 767-794.
 - [26] A. Bonito, J.P. Borthagaray, R.H. Nochetto, E. Otárola, A.J. Salgado, Numerical methods for fractional diffusion, *Comput. Vis. Sci.*, 19(5-6) (2018), pp. 19-46.
 - [27] S. Arshad, J. Huang, A.Q.M. Khaliq, Y. Tang, Trapezoidal scheme for time-space fractional diffusion equation with Riesz derivative, *J. Comput. Phys.*, 350 (2017), pp. 1-15.
 - [28] S. Arshad, W. Bu, J. Huang, Y. Tang, Y. Zhao, Finite difference method for time-space linear and nonlinear fractional diffusion equations, *Int. J. Comput. Math.*, 95(1) (2018), pp. 202-217.
 - [29] X.-M. Gu, T.-Z. Huang, C.-C. Ji, B. Carpentieri, A.A. Alikhanov, Fast iterative method with a second-order implicit difference scheme for time-space fractional convection-diffusion equation, *J. Sci. Comput.*, 72(3) (2017), pp. 957-985.
 - [30] L.B. Feng, P. Zhuang, F. Liu, I. Turner, Y.T. Gu, Finite element method for space-time fractional diffusion equation, *Numer. Algorithms*, 72(3) (2016), pp. 749-767.
 - [31] X.Q. Yue, W.P. Bu, S. Shu, M.H. Liu, S. Wang, Fully finite element adaptive AMG method for time-space Caputo-Riesz fractional diffusion equations, *Adv. Appl. Math. Mech.*, 10(5) (2018), pp. 1103-1125.
 - [32] T.A. Biala, A.Q.M. Khaliq, Parallel algorithms for nonlinear time-space fractional parabolic PDEs, *J. Comput. Phys.*, 375(2018), pp. 135-154.
 - [33] S. Duo, L. Ju, Y. Zhang, A fast algorithm for solving the space-time fractional diffusion equation, *Comput. Math. Appl.*, 75(6) (2018), pp. 1929-1941.
 - [34] Y. Hu, C. Li, H. Li, The finite difference method for Caputo-type parabolic equation with fractional Laplacian: One-dimension case, *Chaos Soliton Fract.*, 102 (2017), pp. 319-326.
 - [35] Y. Hu, C. Li, H. Li, The finite difference method for Caputo-type parabolic equation with fractional Laplacian: more than one space dimension, *Int. J. Comput. Math.*, 95(6-7) (2018), pp. 1114-1130.
 - [36] Y. Huang, A. Oberman, Numerical methods for the fractional Laplacian: A finite difference-quadrature approach, *SIAM J. Numer. Anal.*, 52(6) (2014), pp. 3056-3084.
 - [37] S. Duo, H.W. van Wyk, Y. Zhang, A novel and accurate finite difference method for the fractional

- Laplacian and the fractional Poisson problem, *J. Comput. Phys.*, 355 (2018), pp. 233-252.
- [38] S. Duo, Y. Zhang, Accurate numerical methods for two and three dimensional integral fractional Laplacian with applications, *Comput. Meth. Appl. Mech. Eng.*, 355 (2019), pp. 639-662.
- [39] Z. Hao, Z. Zhang, R. Du, Fractional centered difference scheme for high-dimensional integral fractional Laplacian, *ResearchGate preprint*, 17 Sept. 2019, 19 pages. DOI: 10.13140/RG.2.2.27556.42889.
- [40] A. Bonito, W. Lei, J.E. Pasciak, Numerical approximation of the integral fractional Laplacian, *Numer. Math.*, 142(2) (2019), pp. 235-278.
- [41] G. Acosta, J.P. Borthagaray, O. Bruno, M. Maas, Regularity theory and high order numerical methods for the (1D)-fractional Laplacian, *Math. Comp.* 87(312) (2018), pp. 1821-1857.
- [42] G. Acosta, F.M. Bersetche, J.P. Borthagaray, A short FE implementation for a 2d homogeneous Dirichlet problem of a fractional Laplacian, *Comput. Math. Appl.*, 74(4) (2017), pp. 784-816.
- [43] V. Minden, L. Ying, A simple solver for the fractional Laplacian in multiple dimensions, *arXiv preprint*, arXiv:1802.03770, 6 Aug. 2018, 25 pages.
- [44] Y. Lin, C. Xu, Finite difference/spectral approximations for the time-fractional diffusion equation, *J. Comput. Phys.*, 225(2) (2007), pp. 1533-1552.
- [45] Q. Guan, M. Gunzburger, θ schemes for finite element discretization of the space-time fractional diffusion equations, *J. Comput. Appl. Math.*, 288 (2015), pp. 264-273.
- [46] Z. Liu, A. Cheng, X. Li, H. Wang, A fast solution technique for finite element discretization of the space-time fractional diffusion equation, *Appl. Numer. Math.*, 119 (2017), pp. 146-163.
- [47] A. Chen, Q. Du, C. Li, Z. Zhou, Asymptotically compatible schemes for space-time nonlocal diffusion equations. *Chaos Soliton Fract.*, 102 (2017), pp. 361-371.
- [48] R.H. Chan, M.K. Ng, Conjugate gradient methods for Toeplitz systems, *SIAM Rev.* 38(3) (1996), pp. 427-482.
- [49] M.K. Ng, *Iterative Methods for Toeplitz Systems*, Oxford University Press, New York, NY (2004).
- [50] S.-L. Lei, H.-W. Sun, A circulant preconditioner for fractional diffusion equations, *J. Comput. Phys.*, 242 (2013), pp. 715-725.
- [51] K. Sakamoto, M. Yamamoto, Initial value/boundary value problems for fractional diffusion-wave equations and applications to some inverse problems, *J. Math. Anal. Appl.*, 382(1) (2011), pp. 426-447.
- [52] J.-Y. Shen, Z.-Z. Sun, R. Du, Fast finite difference schemes for time-fractional diffusion equations with a weak singularity at initial time, *East Asian J. Appl. Math.*, 8(4) (2018), pp. 834-858.
- [53] R.H. Nochetto, E. Otárola, A.J. Salgado, A PDE approach to space-time fractional parabolic problems, *SIAM J. Numer. Anal.*, 54(2) (2016), pp. 848-873.
- [54] S. Jiang, J. Zhang, Q. Zhang, Z. Zhang, Fast evaluation of the Caputo fractional derivative and its applications to fractional diffusion equations, *Commun. Comput. Phys.*, 21(3) (2017), pp. 650-678.
- [55] H.-K. Pang, H.-W. Sun, Multigrid method for fractional diffusion equations, *J. Comput. Phys.*, 231(2) (2012), pp. 693-703.
- [56] R.A. Horn, C.R. Johnson, *Matrix Analysis* (2nd ed.), Cambridge University Press, New York, NY (2012).
- [57] X.-L. Lin, M.K. Ng, A fast solver for multidimensional time-space fractional diffusion equation with variable coefficients, *Comput. Math. Appl.*, 78(5) (2019), pp. 1477-1489.
- [58] H.A. van der Vorst, Bi-CGSTAB: A fast and smoothly converging variant of Bi-CG for the solution of nonsymmetric linear systems, *SIAM J. Sci. Stat. Comput.*, 13(2) (1992), pp. 631-644.